HHS Public Access

Author manuscript

FEBS Lett. Author manuscript; available in PMC 2019 November 01.

Published in final edited form as:

FEBS Lett. 2018 November ; 592(21): 3542–3562. doi:10.1002/1873-3468.13160.

The fusion pore, 60 years after the first cartoon

Satyan Sharma[1] and **Manfred Lindau**[1,2]

[1]Laboratory for Nanoscale Cell Biology, Max-Planck-Institute for Biophysical Chemistry, Göttingen, Germany

[2]School of Applied and Engineering Physics, Cornell University, Ithaca, New York, USA

Abstract

Neurotransmitter release occurs in the form of quantal events by fusion of secretory vesicles with the plasma membrane, and begins with the formation of a fusion pore that has a conductance similar to that of a large ion channel or gap junction. In this review we propose mechanisms of fusion pore formation and discuss their implications for fusion pore structure and function. Accumulating evidence indicates a direct role of SNARE proteins in the opening of fusion pores. Fusion pores are likely neither protein channels nor purely lipid, but are of proteolipidic composition. Future perspectives to gain better insight into the molecular structure of fusion pores are discussed.

Introduction

The first report indicating that synaptic transmission occurs in the form of discrete packages of neurotransmitter was published by Fatt and Katz in Nature (1950) with the title "*Some observations on biological noise*". When they recorded from frog muscle fibers, they observed that "when the electrode is inserted immediately under the motor nerve endings … there is local activity of a characteristic nature: small action potentials of rapid rise and slow decay follow one another at random intervals. These discharges occur in discrete sizes, indicative of a number of separately firing units." and they concluded "We must therefore think of a local mechanism by which acetylcholine [(Ach)] is released at random moments, in fairly large quantities;.." [1]. A few years later the first electron micrographs of synapses were published showing small membrane bound microsomes in the presynaptic nerve terminals that were named synaptic vesicles [2].

Inspired by the discovery of the synaptic vesicles, Del Castillo and Katz presented at an International CNRS Colloquium entitled *Microphysiologie Comparée des Éleménts Excitables* in 1955 the vesicular hypothesis of neurotransmitter release. In the landmark paper entitled "*La base <quantale> de la transmission neuro-musculaire*" published in the proceedings from this colloquium [3] they presented the scheme shown in Fig. 1. In translation, the figure legend states "***The transmitter is believed to be preformed in intracellular microsomes, which after critical collision with the nerve membrane, release their Ach contents into the intersynaptic space…..it can be assumed that it occurs when certain reactive molecules (represented by dots) of the two surfaces meet***." With remarkable intuition they suggest in this scheme that when the reactive molecules meet, a small pore is opened allowing for escape of Ach.

Combining rapid freezing with electron microscopy, Heuser and Reese captured fusing vesicles in the frog neuromuscular junction, which revealed omega-shaped structures with membrane lined pores of ~20 nm diameter [4]. Because of their large diameter and smoothness of the membrane lining the pores, these fusion pores seemed to be entirely lipidic but they were thought to be possibly preceded by smaller pores that could not be resolved in these experiments. Information about the initial formation and expansion of fusion pores while their size is < 20 nm, corresponding to the dots in Fig. 1, has been assessed in real time by electrophysiological, electrochemical and fluorescence techniques.

Main Text

Fusion pore conductance and fusion pore structure

Conductances of initial fusion pores indicate molecular dimensions—

Exocytotic fusion of individual vesicles with the plasma membrane leads to an increase in membrane area, which manifests itself as a stepwise capacitance increase in electrophysiological recordings [5]. The first experimental characterization of the initial fusion pore properties was performed by electrophysiological measurements of fusion pore conductance in beige mouse mast cells, which have exceptionally large secretory granules. Due to the large membrane capacitance of large secretory granules it is possible to measure the currents through the fusion pore in whole cell patch clamp experiments [6–8] as illustrated in Fig. 2. Upon fusion pore formation this current charges the granule membrane to the same potential that is set on the plasma membrane by the voltage clamp and the conductance of the nascent fusion pore could be determined with a time resolution of ~20 μs [7]. The experiments revealed an average initial fusion pore conductance of 230–330 pS [6,7], similar to that of a large ion channel or gap junction. However, in contrast to typical ion channels, the conductance varied considerably between individual fusion pore openings [7]. Such measurements were also performed in horse eosinophils, which have similarly large granules and provided similar results [8]. These current transients are brief and provide the time course of fusion pore conductance over the first millisecond of its existence. They show that after the instantaneous opening, the fusion pore conductance begins to rise slowly, indicating fusion pore expansion. On a slower time scale the fusion pore conductance can be determined by admittance analysis using a lock-in amplifier (Fig. 3) [9], which reveals a fluctuating fusion pore conductance [7,10] that may proceed to unmeasurably large conductance that was interpreted as an indication of full fusion. Closing of the fusion pore is indicated by a transient capacitance flicker [5].

For cells with smaller secretory vesicles, the charging currents are too fast to be resolved but fusion pore conductance measurements can be performed using cell attached patch clamp capacitance measurements and admittance analysis [11,12] (Fig. 4). In these measurements the time resolution is lower, providing initial fusion pore conductance values within ~5 ms [13]. Such measurements revealed similar mean initial conductance values in neutrophils (150 pS) [11], chromaffin cells (330 pS) [13–15], and for large dense core vesicles in pituitary nerve terminals (213 pS) [16]. For small vesicles in these nerve terminals [16] and for synaptic vesicles [17], fusion pore conductances have been resolved only during flickering fusion events and the detected fusion pore conductance values were generally

smaller (<45 pS in pituitary nerve terminals and <250 pS in synapses). However, the lack of larger fusion pore conductance values is likely due to the detection limit that makes it extremely difficult to detect fusion pore conductances >50 pS for 50 nm vesicles with only 80 aF capacitance.

Another method to measure individual fusion pore openings uses carbon fiber microelectrodes (CFMs) placed close to a cell that releases oxidizable transmitter, such as catecholamines). Quantal release events produce amperometric spikes that reflect the flux of transmitter release from individual vesicles [18]. These amperometric spikes are often preceded by a so-called foot signal indicating initial slow leakage of catecholamines (Fig. 5) [19].

In chromaffin cells, cell attached patch clamp capacitance measurements were combined with simultaneous measurements of catecholamine release from the same vesicle with a carbon fiber microelectrode inserted into the patch pipette [14,20]. These measurements revealed that the flux of transmitter release through the early fusion pore is proportional to fusion pore conductance [13,14] (Fig. 6). The release of positively charged catecholamines through a narrow fusion pore is an electrodiffusion process associated with entry of sodium ions into the vesicle [13]. The mean proportionality factor is ~10 pA/nS, which means that the amperometric foot current through a 250 pS fusion pore is on average ~2.5 pA. The proportionality factor varies, however, from cell to cell [13] presumably due to cell to cell variability of vesicular catecholamine concentrations [21]. Nevertheless, analysis of amperometric foot currents does provide valuable information about average fusion pore properties and the kinetics of fusion pore dynamics.

Transmitter release is extremely fast, which has led to the hypothesis that it occurs through opening of a pre-assembled fusion pore [22]. Based on the finding that fusion pore conductances were similar to those of ion channels, it was suggested that the fusion pore could be a proteinaceous channel traversing the vesicle membrane and the plasma membrane, similar to a gap junction as shown in Fig. 7 [22,23], which would be able to change conformation very fast and thereby achieve the required speed.

Fusion pore conductance and fusion pore geometry—Measurements of fusion pore conductance have led to predictions of the initial fusion pore geometry. For a cylindrical aqueous pore with radius r, filled with a solution with specific resistivity ρ_{bulk}, its conductance is given by

$$G_P = \frac{\pi r^2}{\rho_{bulk}\left(l + \frac{\pi r}{2}\right)} \quad (1)$$

In the denominator the pore length is increased by $\pi r/2$, a minor correction to account for the access resistance, which relates to the contribution made by the diffusion of ions to the pore mouth (equation 11-1 in ref [24]). Assuming a gap junction-like fusion pore traversing

vesicle and plasma membrane with length l~15 nm and ρ_{bulk}~100 Ωcm, a fusion pore conductance of 250 pS corresponds to a fusion pore radius r~1 nm [6,23].

Equation (1) holds, however, only for large pores, as it does not take into account the interaction of the molecules filling the pore with the pore walls. These interactions lead to a significant reduction of the effective diffusion coefficient of water and ions in a narrow pore. This has been studied by molecular dynamics simulations for the OmpF porin channel, in which the pore radius varies along the length of the pore (z) from ~0.5 nm to ~1.5 nm [25,26], showing a reduced water self-diffusion coefficient giving a correspondingly increased resistivity

$$\rho_{channel}(z) = \rho_{bulk}(D_{bulk}/D_z(z)) \quad (2)$$

where $D_z(z)$ is the diffusion coefficient as a function of the z coordinate along the length of the pore. The ratio $D_z(z)/D_{bulk}$ decreases from ~0.7 at 1.5 nm pore radius to ~0.2 at 0.5 nm pore radius with ~0.5 at 1 nm pore radius [25]. Taking this correction into account increases the radius of a 250 pS fusion pore to ~1.5 nm.

However, as mentioned above, initial fusion pore conductances vary considerably, which differs from the typical behavior of ion channels and gap junctions. One alternative model postulates the formation of a purely lipidic fusion pore, which is to be formed through the remote action of proteins, which are not integral parts of the fusion pore [27–30]. In these models the merging of the membranes proceeds through formation of a stalk and hemifusion intermediate [31,32]. Such lipidic fusion pores were modeled assuming a toroid structure formed by revolving semi-circles that form a pore with a shape resembling the hole in a doughnut (Fig. 8). Such pores could also have conductances consistent with experimental values [27]. Using equation 2 we estimate for a 250 pS pore in a single 4 nm thick bilayer as in Fig. 8C, a pore radius of ~0.6 nm. Evidently, the initial fusion pore conductance would be consistent with both models, giving in both cases a fusion pore with molecular dimensions.

It was suggested that the forces that are necessary to generate tension and curvature leading to a hemifusion intermediate and subsequently pore formation in the hemifusion diaphragm would be generated by a protein scaffold surrounding the fusion site [29] but there is no model of the nanomechanical force generation and its transmission to the membrane contact area. For force transmission, the associated proteins must be very close to the fusion site and must be membrane anchored, making it likely that they also participate somehow in the fusion pore formation. The mechanisms of Figs. 2 and 3 appear to be extreme models. As is often the case, the truth seems to be in between, the formation of a protelipid initial fusion pore [33].

The role of SNARE proteins in fusion pore opening

With the discovery of the SNARE proteins as essential components of the vesicle fusion mechanism [34] and the demonstration that they can form a minimal fusion machinery [35], fusion pore models were developed that incorporate the vesicular SNARE proteins

synaptobrevin 2 (vSNARE), and the plasma membrane proteins (tSNAREs) syntaxin 1 and SNAP25 as integral components. The SNARE proteins turn out to be at least in part the ***reactive molecules (represented by dots)*** (Fig. 1) of the vesicular hypothesis put forward by Del Castillo and Katz [3].

The central importance of the SNARE proteins in fusion pore formation has been evident from the botulinum and tetanus toxins that cleave the SNARE proteins at specific sites and strongly inhibit fusion pore formation [36]. Synaptobrevin 2 and syntaxin 1 are both anchored in the respective membrane by a single transmembrane (TM) domain whereas SNAP25 is lipid anchored through four palmitoylated cysteines. One helical SNARE domain each from synaptobrevin and syntaxin, and two SNARE domains contributed by SNAP25, form a zippered coiled coil [37]. In the post-fusion state the helical bundle continues throughout the synaptobrevin and syntaxin TM domains [38].

The role of SNARE protein TM domains—Several studies were undertaken to determine if the TM domains of syntaxin and synaptobrevin might line the fusion pore, forming a proteinaceous fusion pore as previously proposed [23]. In these experiments the fusion pore was assessed either by cell attached patch clamp recordings measuring fusion pore conductance or by measuring the rate of catecholamine release by amperometry. Measurements of fusion pore conductances and amperometric foot signals investigating the effect of bulky tryptophan point mutations in the syntaxin TM domain revealed small but significant reductions that showed a helical wheel periodicity and it was suggested that 5–7 syntaxin TM domains might form a fusion pore hemichannel in the plasma membrane [39,40]. Results in subsequent experiments with synaptobrevin TM domain mutations also revealed effects on the fusion pore but the point mutations that influence fusion pore permeation fell along two α-helical faces of the TMD [41]. The evidence for a fusion pore lined by syntaxin and synaptobrevin TM domains as two connected fusion pore hemichannels was therefore not entirely conclusive.

How could SNARE proteins open a fusion pore—The general significance of the SNARE TM domains for the process of fusion pore formation was controversial for some time. When the synaptobrevin or syntaxin TM domains were replaced by lipid anchors, fusion was strongly inhibited or abolished [42–44]. However, for synaptobrevin a lipid that spanned both leaflets could support fusion in an *in vitro* assay, which suggests that the TM part of the vSNARE must interact with both leaflets [42]. Synaptobrevin thus needs a membrane anchor spanning both leaflets of the membrane but the observation that its TM domain can be replaced by a lipid with sufficient length [42], the mutational analysis [41], the improved functionality of a TM domain with its central 16 residues replaced by valines [44], and the finding that two copies of synaptobrevin are sufficient to form a fusion pore [45] indicate that it does not form a pore lined by TM domains but that the membrane anchor does nevertheless play a key role in fusion.

The role of interactions of the synaptobrevin C terminus with the intravesicular leaflet was investigated by expressing constructs with C terminal modifications in mouse embryonal chromaffin cells devoid of endogenous synaptobrevin 2 and cellubrevin [46]. These experiments revealed that addition of polar residues strongly inhibited fusion induced by

flash photolysis of caged calcium, which led to the hypothesis that zippering of the SNARE complex pulls the C terminus of synaptobrevin deeper into the membrane and that this movement of the synaptobrevin TM domain may be required for fusion pore opening [46]. Further insight into this mechanism came from coarse grain molecular dynamics simulations, which showed that the activation energy to translocate the synaptobrevin C terminus deeper into the membrane and thereby detach the C terminus from the lipid head groups was strongly increased by C terminal addition of two lysines [47], a construct that totally abolished fusion experimentally [46]. These results point to motion of the synaptobrevin TM domain in the membrane as a key event to induce fusion pore formation. The energy required to tilt the TM domain through the membrane [47] can be provided by SNARE complex zippering as has been shown by direct nanomechanical measurements using optical tweezers [48]. Coarse grain molecular dynamics simulations have shown that tilting the C termini into the hydrophobic core can trigger formation of a fusion pore between two 20 nm vesicles [49].

In addition to the C terminus, the nanomechanical properties of the synaptobrevin TM domains are important. The introduction of helix-stabilizing leucines within the synaptobrevin TM domain impairs exocytosis and delays fusion pore dilation. In contrast, increasing the number of helix-destabilizing, ss-branched valines or isoleucines supports fusion rates just like wild type synaptobrevin but in addition accelerates fusion pore expansion [44]. These results indicated that conformational flexibility of the synaptobrevin-2 TM domain increases fusion rates and accelerates fusion pore expansion.

Evidence for a proteolipid fusion pore incorporating SNARE TM domains— Botulinum toxin A., which cleaves off the 9 C terminal residues of SNAP25 [50,51] inhibits fusion only partially [36,52,53]. Expression of truncated SNAP25, lacking the 9 C terminal residues (SNAP25Δ9) reduces the rate of release events and slows down the kinetics of release from individual vesicles [53,54]. Fusion pores formed by SNAP25Δ9 or by SNAP25 carrying a mutation of R198 to an uncharged or negatively charged residue have lower conductance and produce correspondingly smaller amperometric foot signals, indicating a change in fusion pore structure [54]. The SNAP25 C terminus contributes to the final tight SNARE complex zippering [55,56] but is not located in the membranes, these findings suggest that SNARE proteins and lipids interact to form a proteolipid fusion pore structure (Fig. 9). Strong support for this hypothesis has come from *in vitro* experiments studying SNARE mediated fusion between liposomes and nanodiscs (NDs) [45].

NDs are self-assembled particles, which contain a single phospholipid bilayer stabilized by an encircling membrane scaffold protein. Nanodiscs incorporating synaptobrevin fuse with small unilamellar vesicles containing syntaxin and SNAP25 [57]. While lipid mixing was observed when the synaptobrevin TM domain was replaced by a membrane spanning lipid or with the TM domain of platelet-derived growth factor receptor, a fusion pore life time sufficient for efficient release of vesicle contents required the native synaptobrevin TM domain [57]. Fusion was observed using nanodiscs as small as 6 nm, which is too small to accommodate a lipidic fusion pore [45]. However, a fusion pore formed by SNARE TM domains could also be excluded because fusion was observed with nanodiscs containing as few as 2 copies of synaptobrevin [45] and two v-SNAREs are too few to form a

proteinaceous pore lined by Syb2 TM domains, which would require at least 3 TM domains. Therefore, these results support the formation of a proteolipid pore.

Variable numbers of SNARE complexes determine fusion pore properties—It is widely believed that in synaptic vesicles or dense core granules fusion pore formation involves more than one SNARE complex. Synaptic vesicles contain ~70 copies of synaptobrevin [58], but it is unclear how many of these cooperate in the formation of a fusion pore [59]. *In* vitro experiments indicated that one SNARE complex is sufficient for fusion as indicated by lipid mixing [57,60], more are needed to produce a fusion pore that is stable enough to allow for efficient cargo release. Apparently, more SNAREs are required for efficient fusion of large vesicles while fewer can support maximal fusion rates of small (40 nm) vesicles [61]. An imaging study suggested a minimal requirement of two copies of synatobrevin for synaptic vesicle fusion and transmitter release [62]. At least three copies of SNAP-25 appear to be required for fast fusion in chromaffin cells [63]. It has been suggested that the fusion rate may increase with increasing numbers of SNARE complexes and that activation of fusion within 1 ms may require a cluster of at least 15 SNARE complexes [64]. These results suggest that fusion pores may be formed by a variable number of SNARE complexes leading to fusion pore properties that depend on this number.

Experiments combining total internal reflection fluorescence (TIRF) imaging of a SNAP25 FRET construct with amperometric imaging by a 4-electrode electrochemical detector array showed that fusion sites associated with a SNAP25 cluster produced amperometric spikes without a foot signal whereas sites lacking such a cluster produced amperometric spikes that were preceded by a foot signal [65]. These results suggest that fusion pores that originate at a tSNARE cluster and presumably involve a larger number of SNARE complexes, expand rapidly whereas those involving fewer SNARE complexes exhibit delayed fusion pore expansion. Measurements of fusion pore conductance using v-SNARE-containing NDs as fusion partners with cells expressing ‘flipped’ t-SNAREs in their plasma membrane showed that fusion pore formation required a minimum of two v-SNAREs per ND face. These pores show a flickering behavior and, presumably due to their constriction in the ND, eventually close again. The average conductance of these flickers increased with increasing number of v-SNAREs in the NDs and was ~450 pS for NDs with 8 v-SNARES but was ~2,200 pS for NDs carrying 30 v-SNAREs. The increased pore dilation with increasing v-SNARE copies was not saturated at 15 v-SNARE copies per face, which was the maximum capacity of the 23 nm NDs used in these experiments [66]. Consistent with these results, fusion pore size increased from ~1 nm to ~3 nm with increasing SNARE copy numbers from 3 to 7, based on electrophysiological ND-planar membrane fusion pore conductance measurements [67].

The dynamics of fusion pore expansion

The lifetime of narrow fusion pores ranges from tens of microseconds to hundreds of milliseconds depending on the type of cell and vesicle being considered. While in many cases the fusion pore proceeds to an expanded state, an alternative outcome is the closing the fusion pore, which may limit release to a fraction of the vesicle contents. A fusion pore expanding from an initial conductance of 165 pS could expand to ~8,000 pS conductance and still close again [7] and vesicle membrane area may change during transient fusion pore

opening [68]. The closure of expanded fusion pores is thus not an exact reversal of the steps that open and expand the fusion pore.

Deletion of the last 9 residues of SNAP-25 in the SNAP25Δ9 construct or the mutations R198Q, R198E, and K201E increase the lifetime of narrow fusion pores and amperometric foot signals, indicating delayed fusion pore expansion [54]. Extending the synaptobrevin linker region, which connects its SNARE domain to its TM domain, also delays fusion pore expansion [69]. In contrast, the synaptobrevin mutations L84A and L84N located in the interaction layer +8 of the SNARE complex accelerate fusion pore expansion [70]. These C terminal interactions of the SNARE domains contribute to the final tight SNARE complex zippering [55,56] and extending the linker weakens the transmission to the TM domains, which suggests that SNARE complex zippering may directly contribute forces not only to fusion pore formation but also towards fusion pore expansion.

More expanded states of the fusion pore have a conductance too large to be measured and are not identified by an amperometric foot current. These states and their dynamic changes have been investigated in live cells using imaging techniques. In neuroendocrine cells, the Ω shapes formed by vesicle fusion are often very stable. While lipid probes, such as styryl FM dyes, diffuse very rapidly into the plasma membrane after fusion pore formation [71,72], this is not the case for vesicle membrane proteins such as phogrin [73], indicating that different components of the vesicle membrane exchange differentially with the plasma membrane. Also the fluorescent membrane label 1,1′-dioctadecyl-3,3,3′,3′ tetramethylindo-carbocyanine perchlorate (diI) [74], rapidly diffuses from the plasma membrane into the granule membrane [75], confirming the rapid lipid exchange between granule membrane and plasma membrane.

Regulation of fusion pore dynamics—Electrophysiological and amperometric studies on mast cells and eosinophils have shown that elevating $[Ca^{2+}]_i$ increases the fusion pore expansion rate while initial fusion pore conductance is not affected [8,76]. In chromaffin cells the frequency of flickers during amperometric foot signals increases with increasing $[Ca^{2+}]_i$ indicating increased fluctuations of fusion pore conductance [77]. $[Ca^{2+}]_i$ thus regulates not only fusion pore formation but also its subsequent dynamics. Strongly elevated extracellular $[Ca^{2+}]$ shifts the mode of exocytosis to the kiss-and-run mechanism but this may also reflect interactions of extracellular Ca^{2+} ions entering the vesicle through the fusion pore with the granular matrix [78].

Vesicle fusion involves various accessory proteins in addition to the SNAREs (Fig. 9). The most studied Ca^{2+} sensor is synaptotagmin 1 (Syt1), which mediates fast synchronous transmitter release [79]. In PC12 cells, overexpression of Syt1 prolonged amperometric foot signals and thus the time from fusion pore opening to dilation, whereas synaptotagmin IV shortened this time [80]. Syt1 mutations that reduced its binding to SNAREs also showed a reduction in foot duration [81]. Corresponding results were obtained with Syt1/Syt9 knock-down [82], suggesting that Syt1 as well as other Syt isoforms regulate fusion pore dynamics. Amperometric recordings from Syt7 knockout chromaffin cells showed a reduced rate of fusion events but no change in quantal size and foot duration suggesting that these are mediated by Syt1. However, in patch amperometry recordings, which selectively measures

fusion pores with very long duration, the duration was further increased in the Syt7 knockout, suggesting that Syt7 plays a role in the subset of fusion pores that expand after a long delay [83]. Interestingly Syt1 and Syt7 are mostly localized in separate granule populations in chromaffin cells. Polarized TIRF experiments indicated full fusion and fast release of fluorescently tagged neuropeptide Y (NPY) from Syt1 granules whereas Syt7 granules showed slow release and extended stability of Ω-shaped vesicles connected to the plasma membrane by an open fusion pore [84]. These results are consistent with the unchanged properties of Syt7 independent short foot signals associated with rapid release and the delayed fusion pore expansions involving Syt7 [83]. It remains to be determined what Syt1 isoform (if any) mediates fusion of Syt7 granules in the absence of Syt7 where fusion pore expansion is delayed even further. Switching the C2B Ca^{2+}-binding loops of Syt1 to those of Syt7 also exhibited slower fusion pore expansion and neuropeptide release relative to wild type Syt1 [85]. There is thus strong evidence for a role of Syt1 and its homologs in fusion pore dynamics.

Expression of a Munc18-1 mutant with reduced affinity for syntaxin in chromaffin cells shortened the duration of amperometric spikes and decreased quantal size suggesting a shift to kiss-and-run fusion [86] but this result was not confirmed in a later study [87]. Regulation of fusion pore dynamics by complexin is similarly controversial [88,89]. A recent study suggested antagonistic effects of complexin and synaptotagmin. Complexin II deficiency was without effect on fusion pore dynamics at high $[Ca^{2+}]_i$, but accelerated fusion pore expansion at low $[Ca^{2+}]_i$. Conversely, over expression of complexin II delayed fusion pore expansion as did deletion of Syt1 [90].

Disease related fusion pore regulation—Alpha-synuclein is a presynaptic protein implicated in Parkinson's disease pathogenesis. It is localized on dense core vesicles and accelerates the kinetics of individual release events of brain derived neurotrophic factor (BDNF) labeled with pHluorin and reduces fusion pore closure ('kiss-and-run') [91]. Mutations that cause Parkinson's disease abrogate this property without impairing its ability to inhibit exocytosis when overexpressed [91], indicating that the pathogenesis of Parkinson's disease may be related to changes in fusion pore dynamics.

Amisyn is a syntaxin binding protein and its overexpression increases the foot duration, indicating more persistent fusion pore restriction [92]. A mutant form of the transcription factor *SOX4* that is implicated in type 2 diabetes, upregulates the expression of amisyn and thereby changes fusion pore properties in beta cells [93]. It was suggested that increased SOX4 expression inhibits insulin secretion and increased diabetes risk by the upregulation of amisyn and an increase in kiss-and-run exocytosis with restricted fusion pore size that impairs insulin release. It was proposed that pharmacological interventions promoting fusion pore expansion may be effective in diabetes therapy [93].

Fusion pore expansion dynamics depends on vesicle content—The release of different granular contents from Ω-shaped fused vesicles shows different kinetics. Catecholamine release measured by amperometry is generally very rapid with a half time <10 ms [18]. NPY and tissue plasminogen activator (tPA) are endogenously expressed proteins in bovine chromaffin cell granules but are present in distinct subpopulations [94].

While release of fluorescently labeled NPY is generally also rapid (<200 ms), release of tPA takes many seconds [95]. Polarized TIRF imaging revealed that ~70% of fusion events of tPA-cerulean-containing granules maintained Ω shape curvature for >10 s, about half of them appeared connected to the plasma membrane by a short narrow neck. Such persistent shapes were not commonly observed upon fusion of granules containing NPY-cerulean [96]. In dense core granules of cortical neurons, similar differences between release of NPY and tPA were reported with release of semaphorin 3A and BDNF resembling the features of tPA release [97]. The persistent Ω shapes are strongly diminished when the interactions between the cargo molecules and the granular matrix are abolished [97]. It would be interesting to know if these differential fusion properties with respect to granule cargo are related to the differential localization of Syt1 and Syt7 discussed in the preceding section.

Plasminogen activator inhibitor (PAI), the physiological inhibitor of tPA, is coexpressed in secretory granules and co-discharged with tPA. The persistent Ω shape creates a nanoscale reaction chamber in which tPA may be inhibited in response to the pH increase in this compartment following fusion pore formation [98]. Thereby the release of enzymatically active tPA is reduced and the covalent tPA/PAI complex is released instead. This complex may have physiological function as it is a high affinity ligand for the LDL receptor-related protein LRP-1 [98].

Evidence for shrinking rather than flattening of Ω profiles—Recently, live super-resolution imaging of dense core granule fusion in chromaffin cells has provided impressive direct insight into the real time behavior of expanded fusion pores. Experiments were performed combining confocal and STimulated Emission Depletion (STED) microscopy [99] to image entry of a fluorescent dyes present in the bath solution, release of GFP-labeled NPY (NPY-GFP), and the fate of the GFP labeled vSNARE, VAMP2-GFP [100]. Two dyes were used simultaneously with one excited with very high intensity leading to rapid bleaching if the fusion pore had closed but not if the fusion pore stayed open, allowing rapid exchange with unbleached dye from the extracellular solution. Chromaffin cells were stimulated by 1 s depolarizations in the whole cell patch clamp configuration.

Over the 30 s observation time following the fusion event, these Ω profiles of fused vesicles changed in several different modes. On average, the fusion pore closed during the observation time in about half of the fusion events and remained open in the other half. However, for the Ω shapes studied in these experiments, NPY-GFP was not expressed in most experiments and in view of the results described above, it is possible that different modes may relate to differences in granule cargo or synaptotagmin isoforms as discussed above.

Vesicle flattening, as is widely assumed to occur when the fusion pore expands, was not observed in these experiments. Instead, in ~60% the vesicle was shrinking while an open fusion pore neck persisted. In a significant fraction of the partial shrinking events the fusion pore closed while the partial Ω profile was still present. In the remaining cases, the Ω profile size stayed constant or enlarged while the fusion pore was open. The enlargement would be consistent with the membrane transfer from the plasma membrane to the granule membrane

through the fusion pore during capacitance flickers in mast cells [68] whereas the shrinking would correspond to membrane transfer in the reverse direction.

Interestingly, total VAMP2-GFP fluorescence of the vesicle stayed constant during shrinking while its spot size decreased consistent with it being concentrated around the fusion pore neck. This behavior may explain an old observation in cell-attached patch clamp capacitance measurements in neutrophils showing a gradual capacitance decrease after a capacitance step that started at the time of fusion pore expansion, presumably to a large neck [101]. This capacitance decrease following exocytosis could compensate the capacitance increase from the fusion event partially or completely, as if some of the vesicle membrane would disappear from the Ω profile without entering the plasma membrane, being “sucked up” somehow, eliminating its contribution to the membrane area. It should be noted, however, that previous studies had indicated that only 10% of fusing vesicles retained VAMP2-GFP while in 90% of vesicles rapid loss of VAMP2-GFP occurred by diffusion into the plasma membrane [102]. A possible explanation for such differences could be that the preferred mode of exocytosis appears to depend on the stimulation protocol [103] and on the specific vesicle cargo [95–97].

A role for actin and myosin II—The study by Wen et al indicates that the shrinking of the vesicles is the dominant mode of exocytosis in chromaffin cells when cells were stimulated with a train of ten 50 ms depolarizations [103]. Shrinking was inhibited by hypertonic solution, indicating that it depends on plasma membrane tension. Inhibiting actin polymerization with Latrunculin A or cytochalasin D inhibited vesicle shrinking, which could be partly rescued by hypotonic solution restoring membrane tension. Shrinking was also inhibited in β-actin knock-out cells and rescued by expression of β-actin-GFP. These results are consistent with a previous report demonstrating that actin and myosin II facilitate release from individual chromaffin granules possibly through generation of mechanical forces [104]. Inhibition of myosin II function or actin polymerization both slow down rapid catecholamine release during amperometric spikes [104]. However, the early fusion pore expansion is only delayed by inhibition of actin polymerization but not by the myosin II inhibitor blebbistatin. It was suggested that the relaxation of membrane tension exerted by inhibiting actin polymerization may be responsible for the slower fusion pore expansion [104]. The slower catecholamine release during amperometric spikes due to inhibition of actin polymerization or myosin II function could be by due to matrix compression or by expanding the fusion pore to much larger size. Imaging Lifeact-GFP showed that additional actin was recruited to some of the Ω profiles but this recruitment appeared to lag behind the shrinking, suggesting that the shrinking may not be a consequence of compression [103]. It would be interesting to see if the shrink mode depends on myosin II. The interaction of the secretory granules with actin filaments may be to be mediated by the adaptor molecules N-Wasp and ARP2/3 [105]. Accordingly, wikostatin, which inhibits N-WASP-mediated Arp2/3 dependent F actin assembly inhibited the shrink mode [103].

The fusion pore closures were prominent in cells with large calcium currents and progressively reduced as calcium currents decreased, consistent with the high abundance of rapid kiss-and-run fusion events [106] in cell attached recordings of fusion and transmitter release from chromaffin cells with high calcium concentrations in the pipette solution [78].

Fusion pore closures were also strongly diminished in imaging experiments with the dynamin inhibitor dynasore or a dynamin inhibitory peptide. These results indicate that the observed fusion pore closure involved dynamin activity and was not a reversal of the steps opening the fusion pore [100].

A recent more detailed study using STED microscopy succeeded with imaging of the Ω profiles visualizing fusion pores with 65–490 nm diameter in live cells [107] by expressing mNeonGreen labeled phospholipase Cδ1 PH domain, which labels PIP_2, a lipid that is specifically localized in the cytoplasmic leaflet of the plasma membrane. When the granule fuses with the plasma membrane, the labeled PIP_2 diffuses into the granule membrane allowing improved super-resolution STED imaging of the Ω profile. Smaller fusion pores were also present, as evident from dye entry or release but were below the resolution of the STED images. The images revealed the presence of dynamin surrounding the fusion pore, in support of its role in fusion pore closure. Release of the false transmitter FFN511 [108] was slow when the fusion pore was invisible but fast when a visible expanded fusion pore was present.

It is presently unclear what happens to the dense core matrix in the shrinking vesicles. Given their size, the matrix must either be dissolved or expelled via brief transient expansion of the fusion pore. The latter possibility is supported by the observation of fast NPY-GFP release in most fusion events that were followed by rapid fusion pore closure and in fusion events with rapid shrinking of the vesicle [107]. It is also supported by the observation that rapid and complete release of catecholamines occurred at the end of capacitance flickers in cell-attached patch amperometry experiments [78]. These results indicate that brief transient fusion pore expansion followed by fusion pore closure does not necessarily limit cargo release [78,107].

Do hemifusion intermediates exist?

The question if fusion pore formation occurs from a hemifusion intermediate and is therefore a pore in a single membrane has been intensely debated. The fusion pathway through a hemifusion intermediate was predicted using theoretical approaches in protein-free membranes [109–111] [32]. It was suggested that expansion of the hemifusion intermediate, driven by the bilayer tension, leads to formation of a hemifusion diaphragm (HD), such that a single bilayer separates the fusing compartments. Mathematical modeling of lateral tension versus HD size [112] predicted that the tension at the HD rim may be high enough to cause HD rupture and thus fusion pore formation.

Experimental evidence for hemifusion initially came from studies on viral fusion but was considered to be a dead end pathway that did not lead to fusion pore formation [113–115]. As for hemagglutinin [114], full fusion mediated by SNARE proteins also appears to require a fully membrane spanning synaptobrevin TM domain [42]. Evidence for hemifusion states was also reported in SNARE mediated liposome fusion reconstitution experiments [116,117]. In reconstitution experiments using vesicles incorporating SNARE proteins, extended hemifusion diaphragms were observed and it was suggested that fusion may be initiated at their edges [118]. In a single vesicle–vesicle system with reconstituted SNARE and synaptotagmin-1 proteoliposomes, Ca2+-triggered immediate fusion started from a

membrane–membrane point-contact and proceeded to complete fusion without discernible hemifusion intermediates. In contrast, pathways that involved a stable hemifusion diaphragm only resulted in fusion after many seconds, if at all [119]. Computational molecular dynamics simulations using coarse-grained models predicted a HD for fusion of 15 nm diameter vesicle and indicated that the fusion proceeded via stalk and hemifused intermediates [120]. Atomic-resolution simulations predicted a transition state for vesicle fusion defined by contact of a few lipid tails [121]. A free energy analysis of pore formation pathways in HD using MD simulations showed that the work for fusion pore formation is more favorable for a smaller HD of 1.5 nm radius with a steeper stalk [122]. Simulations of SNARE mediated vesicle fusion using CG MD simulations indicated that fusion pores could be formed quickly through early hemifusion intermediates from a stalk or a stalk could alternatively expand into a HD followed by pore formation initiating at the HD rim [123].

Recent imaging experiments of dense core granule fusion in live chromaffin cells provided evidence for hemi-fused Ω-shaped structures that could proceed to opening of a fusion pore as indicated by dye entry [124], consistent with the *in vitro* results. The transition from a hemifused structure to a fused structure was very slow (seconds to tens of seconds) and occurred in about 1/3 of the observed fusion events. The majority of fusion events occurred without a detectable hemifusion intermediate [124].

These results indicate that for rapid fusion on the time scale of a millisecond or less, a hemifusion intermediate is unlikely and the question arises why a hemifusion intermediate may form in some cases leading to delayed fusion. This question relates to the molecular mechanism of fusion pore opening, which is likely involving a protelipid structure formed by SNARE proteins as well as lipids [33]. For a few SNARE complexes to cooperate in fusion pore formation, they must be located in close proximity. However, zippering of several nearby SNARE complexes likely leads to formation of a ring-shaped arrangement followed by entropically driven radial expansion. This expansion will pull the membranes together with high force depending on the number of SNARE complexes [64]. Given the increased distance between the SNARE complexes, this will likely produce a hemifused zone as observed in the experiments described above. For rapid fusion pore formation a mechanism is presumably needed that keeps the SNARE complexes close together to allow for fusion pore formation before the radial expansion. The subsequent radial expansion will then be the driving force for rapid fusion pore expansion, which will likely depend on the number of SNARE complexes involved.

SNARE complex arrangements limiting their mobility

Role of accessory proteins in fusion pore opening—An extensive body of evidence has shown that accessory proteins in addition to the SNAREs are involved and can substantially accelerate fusion. These proteins include synaptotagmin, complexin, CAPS, Munc18 and Munc13, which are involved in calcium sensing, docking, priming and fusion pore expansion. [80,81,83,86,88,125–130]. Syntaxin and Munc18 were shown to assemble at vesicle docking sites [126]. Together with complexin they form a complex that arrests fusion of docked secretory vesicle that can be primed by CAPS or Munc13 for calcium triggered fusion mediated by synaptotagmin [131]. Very recently, the “buttressed ring

hypothesis" has been put forward, suggesting that an outer ring of up to six curved Munc13 'MUN' domains may surround an inner ring of synaptotagmin C2 domains, forming a structure where SNARE zippering is templated [132]. Such a structure would arrange the SNARE complexes in close proximity, allowing rapid fusion pore formation, while subsequent disassembly of the ring would allow for fusion pore expansion.

It is also possible that dynamin plays a role in expanding SNARE complexes at the fusion site, promoting hemifusion. It has been shown that when dynamin was knocked out or inhibited in chromaffin cells, not only was fusion pore closure inhibited but also the incidence of hemifusion was markedly reduced, shifting the observed mode to fusion pore openings without appearance of hemifusion [124]. The shift towards long-lived Ω shapes by inhibition of dynamin is also consistent with corresponding findings using polarized TIRF imaging [133]. Both studies also find stabilization of Ω shapes when Sr^{++} replaces Ca^{++} during stimulation of fusion [75,124]. This is consistent with the Ca^{++} dependence of fusion pore closure [78,134] and the evidence from interference reflection microscopy that Sr^{++} does not support fusion pore constriction, locking fusion at the Ω shaped open pore state [134].

tSNARE clusters and their function in fusion pore opening—Another mechanism that may prevent premature dissociation of an arrangement of assembled SNARE complexes could be the organization of tSNAREs in clusters [135], which has been reported for PC12 cells [136–138], INS1 cells [126], and neurons [139]. In PC12 cells the tSNARE clusters consist of 50–70 molecules [137,138] and in INS1 cells of ~30; in neurons they consist of at least 10 but possibly many more [139]. tSNARE clusters may be associated with secretory granules (on-granule clusters), but such clusters exist also elsewhere, without associated granules (off-granule clusters). The number of SNAP-25 molecules in these clusters seems similar to that of syntaxin molecules [138]. However, SNAP25 clusters are difficult to identify because, in PC12 cells, SNAP-25 exists in an ~10-fold excess over Syntaxin and the excess SNAP-25 creates rather diffuse background fluorescence [138]. A super-resolution microscopy study using PC12 cells led to the conclusion that the secretory granules do not reside directly over tSNARE clusters but are located between them [140]. Although vesicles with a syntaxin cluster have a higher probability of undergoing exocytosis, vesicles without such a cluster may do so as well. In neurons, t-SNARE clusters showed a high level of colocalization between not only syntaxin and SNAP25 but also Munc-18-1. In the absence of syntaxin1A and knockdown of syntaxin1B, the colocalization of SNAP25 with Munc18-1 was lost [139]. Interestingly, on-granule syntaxin clusters require the syntaxin N terminal H_{abc} domain [141]. In INS1 cells secretory granules were visualized with NPY-mCherry and EGFP-labeled Syntaxin 1, SNAP25, Munc18, Munc13 and rab3a constructs were used to investigate their appearance or dispersal at sites where granules dock, undock or fuse [126]. These experiments revealed that after arrival of a vesicle at the plasma membrane, assembly of a Syntaxin/Munc18 cluster at this site is required to proceed to the docked state. Subsequently, on a time scale of 1–2 minutes SNAP25 and Munc13 appear to be recruited to the docking site [126], presumably preparing the vesicle for fusion in a priming step [142] such that the vesicle can be released rapidly in response to stimulation, i.e. Ca^{2+} entry via voltage-gated Ca^{2+} channels. It is possible that at this stage Munc13 entering the Syntaxin

cluster switches Syntaxin to the open conformation and thereby recruits SNAP-25 to the docking site.

Fusion appears to occur not directly on top of the tSNARE clusters but rather at their edges [143,144]. It has been argued that it is only at the edge where SNAP25 can engage in a complex with syntaxin [144] but this seems to be inconsistent with equal numbers of SNAP25 and syntaxin in the clusters [138]. Recent simulations have shown that at the edge of tSNARE clusters a favorable membrane curvature exists that would allow contact between vesicle and plasma membrane and facilitate fusion pore formation [145]. Fusion pores formed at tSNARE clusters expand more rapidly than those formed in the absence of clusters. [65]

A role for specific lipids

Rapid fusion requires cholesterol: The plasma membrane and secretory vesicles contain ~40% cholesterol [58] and many studies have shown that cholesterol lays a very important role in exocytotic as well as viral fusion (reviewed in [146]). Cholesterol depletion diminishes rapid evoked release and augments spontaneous release in neurons [147]. It also attenuates the frequency of unitary fusion events in lactotrophs [148]. Experiments investigating SNARE-mediated fusion in planar bilayers revealed that increasing cholesterol favors a mechanism of direct fusion pore opening, whereas low cholesterol favors a mechanism leading to a long-lived hemifusion states [149]. One mechanism by which cholesterol may affect fusion pore formation is its effect on spontaneous curvature and elasticity of lipid membranes [150]. However, cholesterol also affects the fusion machinery via its role in tSNARE cluster formation, which was shown to depend on cholesterol [143] in membrane sheets as well as intact cells [151]. Cholesterol depletion leads to loss of syntaxin clusters and inhibition of fusion [135]. In liposome-planar bilayer SNARE mediated fusion experiments, physiological cholesterol levels strongly increased the fraction of fully open fusion pores and fusion pore formation was very rapid, consistent with tSNAREs being preclustered by cholesterol forming functional docking and fusion sites [152].

PIP_2 supports fusion but its role in tSNARE clusters is questionable: Phosphatidylinositol 4,5-bisphosphate (PIP_2) is a minor lipid component localized in the cytoplasmic leaflet of the plasma membrane as well as other organelles and has been implicated as a regulator of in a wide range of membrane proteins (recently reviewed in [153]). PIP_2 interacts with syntaxin via electrostatic interactions [154–156] and depletion of PIP_2 or syntaxin-mutations reducing its PIP_2 interactions inhibit fusion, possibly through a defect in vesicle priming [157–160]. Consistent with these reports, recent experiments have shown that photoactivatable PIP_2 uncaging, which provides a very rapid increase of PIP_2, potentiates exocytosis in mouse chromaffin cells by a mechanism involving synaptotagmin-1 and Munc13-2 as relevant effector proteins. PIP_2 uncaging by itself also triggered rapid fusion of a subset of readily-releasable vesicles [161].

It has been reported that formation of syntaxin clusters depends critically on PI(3,4,5)P3, clustering syntaxin via interactions with its cationic juxtamembrane domain [162]. Also

PIP_2 was found to be associated with syntaxin clusters on the membrane could therefore mediate specific docking of vesicles at cluster sites via synaptotagmin-PIP_2 interactions [145,163–165]. However, these studies were performed in membrane sheets and reconstituted systems and PIP_2 depletion was on a slow time scale. In contrast, rapid PIP_2 reduction in the plasma membrane of INS1 cells strongly inhibited secretion but not sytaxin1a clustering. However, selective local PIP_2 reduction at vesicle docking sites caused vesicle undocking from the plasma membrane at these sites [166]. Another very recent study in live INS1 cells revealed also no evidence for PI(3,4,5)P3 or PIP_2 association with syntaxin clusters and actually no evidence for PIP_2 clustering at all [167]. Instead, PIP_2 appeared to be homogeneously distributed in the plasma membrane. Depletion of PIP_2 had no effect on syntaxin clusters and vesicle docking but, nevertheless, resulted in strong inhibition of exocytosis [167]. It should be noted that PIP_2 clustering, in part associated with syntaxin clusters, was appearing slowly following cell permeabilization [167], suggesting a wash-out phenomenon of some intracellular factor(s) that presumably prevent at least partially the association of PIP_2 with syntaxin clusters in intact cells.

Conclusions and Perspectives

Exocytotic fusion pores have been hypothesized since the formulation of the vesicular hypothesis of neurotransmitter release more than 60 years ago. Since the first fusion pore conductance measurements, which were performed about 30 years ago much has been learned but nevertheless the molecular and nanomechanical details are still largely unknown. The present view is that SNARE proteins and lipids likely form a proteolipid fusion pore but this mechanism involves additional accessory proteins that are required for rapid fusion pore formation. PIP_2 lipids and cholesterol are also important factors that determine vesicle priming and fusion pore properties. In addition fusion pore properties are related and possibly directly affected by vesicle cargo. Given the very transient nature of fusion pores a fusion pore crystal or NMR structure might never be feasible. Thus, significant progress may come from multiscale computer simulations, which can be validated by including experimentally identified molecular manipulations that affect fusion pore properties and that must manifest themselves also in the simulations. In addition advances in utilizing non-natural amino acids might become a tool to investigate the dynamics of molecular interactions on a time scale that relates to that of fusion pore formation.

Acknowledgments

We wish to express our thanks to Annita N. Weis, Ying Zhao, and Qinghua Fang for critical reading and valuable comments on this manuscript. Grant support from the European Research Council (ERC) grant ADG 322699 and US National Institutes of Health (NIH) grant R01GM121787 is gratefully acknowledged.

References

1. Fatt P, Katz B. Some observations on biological noise. Nature. 1950; 166:597–8. [PubMed: 14780165]
2. De Robertis ED, Bennett HS. Some features of the submicroscopic morphology of synapses in frog and earthworm. J Biophys Biochem Cytol. 1955; 1:47–58. [PubMed: 14381427]
3. Del Castillo J, Katz B. La base “quantale” de la transmission neuromusculaire. Colloques Internat CNRS. 1957; 67:245–256.

4. Heuser JE, Reese TS. Structural changes after transmitter release at the frog neuromuscular junction. J Cell Biol. 1981; 88:564–580. [PubMed: 6260814]
5. Fernandez JM, Neher E, Gomperts BD. Capacitance measurements reveal stepwise fusion events in degranulating mast cells. Nature. 1984; 312:453–455. [PubMed: 6504157]
6. Breckenridge LJ, Almers W. Currents through the fusion pore that forms during exocytosis of a secretory vesicle. Nature. 1987; 328:814–817. [PubMed: 2442614]
7. Spruce AE, Breckenridge LJ, Lee AK, Almers W. Properties of the fusion pore that forms during exocytosis of a mast cell secretory vesicle. Neuron. 1990; 4:643–654. [PubMed: 2344404]
8. Hartmann J, Lindau M. A novel Ca(2+)-dependent step in exocytosis subsequent to vesicle fusion. FEBS Lett. 1995; 363:217–20. [PubMed: 7737405]
9. Lindau M. Time-resolved capacitance measurements: monitoring exocytosis in single cells. Q Rev Biophys. 1991; 24:75–101. [PubMed: 2047522]
10. Curran MJ, Cohen FS, Chandlers DE, Munson PJ, Zimmerberg J. Exocytotic fusion pores exhibit semi-stable states. J Membr Biol. 1993; 133:61–75. [PubMed: 8320720]
11. Lollike K, Borregaard N, Lindau M. The exocytotic fusion pore of small granules has a conductance similar to an ion channel. J Cell Biol. 1995; 129:99–104. [PubMed: 7535305]
12. Debus K, Lindau M. Resolution of patch capacitance recordings and of fusion pore conductances in small vesicles. Biophys J. 2000; 78:2983–97. [PubMed: 10827977]
13. Gong LW, de Toledo GA, Lindau M. Exocytotic catecholamine release is not associated with cation flux through channels in the vesicle membrane but Na^+ influx through the fusion pore. Nat Cell Biol. 2007; 9:915–922. [PubMed: 17643118]
14. Albillos A, Dernick G, Horstmann H, Almers W, Alvarez de Toledo G, Lindau M. The exocytotic event in chromaffin cells revealed by patch amperometry. Nature. 1997; 389:509–12. [PubMed: 9333242]
15. Dernick G, Alvarez de Toledo G, Lindau M. Exocytosis of single chromaffin granules in cell-free inside-out membrane patches. Nat Cell Biol. 2003; 5:358–62. [PubMed: 12652310]
16. Klyachko VA, Jackson MB. Capacitance steps and fusion pores of small and large-dense-core vesicles in nerve terminals. Nature. 2002; 418:89–92. [PubMed: 12097912]
17. He L, Wu XS, Mohan R, Wu LG. Two modes of fusion pore opening revealed by cell-attached recordings at a synapse. Nature. 2006; 444:102–5. [PubMed: 17065984]
18. Wightman RM, et al. Temporally resolved catecholamine spikes correspond to single vesicle release from individual chromaffin cells. Proc Natl Acad Sci U S A. 1991; 88:10754–10758. [PubMed: 1961743]
19. Chow RH, Rüden Lv, Neher E. Delay in vesicle fusion revealed by electrochemical monitoring of single secretory events in adrenal chromaffin cells. Nature. 1992; 356:60–63. [PubMed: 1538782]
20. Dernick G, Gong LW, Tabares L, Alvarez de Toledo G, Lindau M. Patch amperometry: high-resolution measurements of single-vesicle fusion and release. Nat Methods. 2005; 2:699–708. [PubMed: 16118641]
21. Gong LW, Alvarez De Toledo G, Lindau M. Secretory vesicles membrane area is regulated in tandem with quantal size in chromaffin cells. J Neurosci. 2003; 23:7917–7921. [PubMed: 12944522]
22. Almers W, Tse FW. Transmitter release from synapses: Does a preassembled fusion pore initiate exocytosis? Neuron. 1990; 4:813–818. [PubMed: 1972885]
23. Almers W. Exocytosis. Annual Reviews of Physiology. 1990; 52:607–624.
24. Hille B. Ionic Channels of Excitable Membranes. Sinauer Associates, Inc; Sunderland, MA: 1992.
25. Smart OS, Coates GM, Sansom MS, Alder GM, Bashford CL. Structure-based prediction of the conductance properties of ion channels. Faraday Discuss. 1999; 111:185–99.
26. Smart OS, Neduvelil JG, Wang X, Wallace BA, Sansom MS. HOLE: a program for the analysis of the pore dimensions of ion channel structural models. J Mol Graph. 1996; 14:354–60. 376. [PubMed: 9195488]
27. Nanavati C, Markin VS, Oberhauser AF, Fernandez JM. The exocytotic fusion pore modeled as a lipidic pore. Biophys J. 1992; 63:1118–1132. [PubMed: 1420930]

28. Chanturiya A, Chernomordik LV, Zimmerberg J. Flickering fusion pores comparable with initial exocytotic pores occur in protein-free phospholipid bilayers. Proc Natl Acad Sci U S A. 1997; 94:14423–8. [PubMed: 9405628]
29. Monck JR, Fernandez JM. The exocytotic fusion pore. J Cell Biol. 1992; 119:1395–1404. [PubMed: 1469040]
30. Monck JR, Fernandez JM. The fusion pore and mechanisms of biological membrane fusion. Curr Opin Cell Biol. 1996; 8:524–33. [PubMed: 8791451]
31. Zimmerberg J, Vogel SS, Chernomordik LV. Mechanisms of membrane fusion. Annu Rev Biophys Biomol Struct. 1993; 22:433–466. [PubMed: 8347997]
32. Kozlovsky Y, Kozlov MM. Stalk model of membrane fusion: solution of energy crisis. Biophys J. 2002; 82:882–95. [PubMed: 11806930]
33. Sharma S, Lindau M. The mystery of the fusion pore. Nat Struct Mol Biol. 2016; 23:5–6. [PubMed: 26733219]
34. Söllner T, Whiteheart S, Brunner M, Erdjument-Bromage H, Geromanos M, Tempst P, Rothman JE. SNAP receptors implicated in vesicle targeting and fusion. Nature (London). 1993; 362:318–323. [PubMed: 8455717]
35. Weber T, Zemelman BV, McNew JA, Westermann B, Gmachl M, Parlati F, Söllner TH, Rothman JE. SNAREpins: minimal machinery for membrane fusion. Cell. 1998; 92:759–772. [PubMed: 9529252]
36. Montecucco C, Schiavo G. Structure and function of tetanus and botulinum neurotoxins. Q Rev Biophys. 1995; 28:423–72. [PubMed: 8771234]
37. Sutton RB, Fasshauer D, Jahn R, Brunger AT. Crystal structure of a SNARE complex involved in synaptic exocytosis at 2.4 Å resolution. Nature. 1998; 395:347–353. [PubMed: 9759724]
38. Stein A, Weber G, Wahl MC, Jahn R. Helical extension of the neuronal SNARE complex into the membrane. Nature. 2009; 460:525–8. [PubMed: 19571812]
39. Han X, Jackson MB. Electrostatic interactions between the syntaxin membrane anchor and neurotransmitter passing through the fusion pore. Biophys J. 2005; 88:L20–2. [PubMed: 15653732]
40. Han X, Wang CT, Bai J, Chapman ER, Jackson MB. Transmembrane segments of syntaxin line the fusion pore of Ca^{2+}-triggered exocytosis. Science. 2004; 304:289–92. [PubMed: 15016962]
41. Chang CW, Hui E, Bai J, Bruns D, Chapman ER, Jackson MB. A structural role for the synaptobrevin 2 transmembrane domain in dense-core vesicle fusion pores. J Neurosci. 2015; 35:5772–80. [PubMed: 25855187]
42. McNew JA, Weber T, Parlati F, Johnston RJ, Melia TJ, Söllner TH, Rothman JE. Close is not enough: SNARE-dependent membrane fusion requires an active mechanism that transduces force to membrane anchors. J Cell Biol. 2000; 150:105–17. [PubMed: 10893260]
43. Chang CW, Chiang CW, Gaffaney JD, Chapman ER, Jackson MB. Lipid-anchored Synaptobrevin Provides Little or No Support for Exocytosis or Liposome Fusion. J Biol Chem. 2016; 291:2848–57. [PubMed: 26663078]
44. Dhara M, et al. v-SNARE transmembrane domains function as catalysts for vesicle fusion. Elife. 2016:5.
45. Bao H, Goldschen-Ohm M, Jeggle P, Chanda B, Edwardson JM, Chapman ER. Exocytotic fusion pores are composed of both lipids and proteins. Nat Struct Mol Biol. 2016; 23:67–73. [PubMed: 26656855]
46. Ngatchou AN, Kisler K, Fang Q, Walter AM, Zhao Y, Bruns D, Sorensen JB, Lindau M. Role of the synaptobrevin C terminus in fusion pore formation. Proc Natl Acad Sci U S A. 2010; 107:18463–8. [PubMed: 20937897]
47. Lindau M, Hall BA, Chetwynd A, Beckstein O, Sansom MSP. Coarse-Grain Simulations Reveal Movement of the Synaptobrevin C-Terminus in Response to Piconewton Forces. Biophys J. 2012; 103:959–969. [PubMed: 23009845]
48. Gao Y, Zorman S, Gundersen G, Xi Z, Ma L, Sirinakis G, Rothman JE, Zhang Y. Single reconstituted neuronal SNARE complexes zipper in three distinct stages. Science. 2012; 337:1340–3. [PubMed: 22903523]

49. Risselada HJ, Kutzner C, Grubmuller H. Caught in the act: visualization of SNARE-mediated fusion events in molecular detail. ChemBioChem. 2011; 12:1049–55. [PubMed: 21433241]
50. Schiavo G, Santucci A, Dasgupta BR, Mehta PP, Jontes J, Benfenati F, Wilson MC, Montecucco C. Botulinum neurotoxins serotypes A and E cleave SNAP-25 at distinct COOH-terminal peptide bonds. FEBS Lett. 1993; 335:99–103. [PubMed: 8243676]
51. Blasi J, et al. Botulinum neurotoxin A selectively cleaves the synaptic protein SNAP-25. Nature. 1993; 365:160–163. [PubMed: 8103915]
52. Wei S, Xu T, Ashery U, Kollewe A, Matti U, Antonin W, Rettig J, Neher E. Exocytotic mechanism studied by truncated and zero layer mutants of the C-terminus of SNAP-25. EMBO J. 2000; 19:1279–89. [PubMed: 10716928]
53. Criado M, Gil A, Viniegra S, Gutierrez LM. A single amino acid near the C terminus of the synaptosomeassociated protein of 25 kDa (SNAP-25) is essential for exocytosis in chromaffin cells. Proc Natl Acad Sci U S A. 1999; 96:7256–61. [PubMed: 10377401]
54. Fang Q, Berberian K, Gong LW, Hafez I, Sorensen JB, Lindau M. The role of the C terminus of the SNARE protein SNAP-25 in fusion pore opening and a model for fusion pore mechanics. Proc Natl Acad Sci U S A. 2008; 105:15388–92. [PubMed: 18829435]
55. Sorensen JB, Wiederhold K, Muller EM, Milosevic I, Nagy G, de Groot BL, Grubmuller H, Fasshauer D. Sequential N- to C-terminal SNARE complex assembly drives priming and fusion of secretory vesicles. EMBO J. 2006; 25:955–66. [PubMed: 16498411]
56. Fang Q, Zhao Y, Herbst AD, Kim BN, Lindau M. Positively Charged Amino Acids at the SNAP-25 C Terminus Determine Fusion Rates, Fusion Pore Properties, and Energetics of Tight SNARE Complex Zippering. J Neurosci. 2015; 35:3230–9. [PubMed: 25698757]
57. Shi L, Shen QT, Kiel A, Wang J, Wang HW, Melia TJ, Rothman JE, Pincet F. SNARE proteins: one to fuse and three to keep the nascent fusion pore open. Science. 2012; 335:1355–9. [PubMed: 22422984]
58. Takamori S, et al. Molecular anatomy of a trafficking organelle. Cell. 2006; 127:831–46. [PubMed: 17110340]
59. Sudhof TC. Neurotransmitter release: the last millisecond in the life of a synaptic vesicle. Neuron. 2013; 80:675–90. [PubMed: 24183019]
60. van den Bogaart G, Holt MG, Bunt G, Riedel D, Wouters FS, Jahn R. One SNARE complex is sufficient for membrane fusion. Nat Struct Mol Biol. 2010; 17:358–64. [PubMed: 20139985]
61. Hernandez JM, Kreutzberger AJ, Kiessling V, Tamm LK, Jahn R. Variable cooperativity in SNARE-mediated membrane fusion. Proc Natl Acad Sci U S A. 2014; 111:12037–42. [PubMed: 25092301]
62. Sinha R, Ahmed S, Jahn R, Klingauf J. Two synaptobrevin molecules are sufficient for vesicle fusion in central nervous system synapses. Proc Natl Acad Sci U S A. 2011; 108:14318–23. [PubMed: 21844343]
63. Mohrmann R, de Wit H, Verhage M, Neher E, Sorensen JB. Fast vesicle fusion in living cells requires at least three SNARE complexes. Science. 2010; 330:502–5. [PubMed: 20847232]
64. Mostafavi H, Thiyagarajan S, Stratton BS, Karatekin E, Warner JM, Rothman JE, O'Shaughnessy B. Entropic forces drive self-organization and membrane fusion by SNARE proteins. Proc Natl Acad Sci U S A. 2017; 114:5455–5460. [PubMed: 28490503]
65. Zhao Y, Fang Q, Herbst AD, Berberian KN, Almers W, Lindau M. Rapid structural change in synaptosomal-associated protein 25 (SNAP25) precedes the fusion of single vesicles with the plasma membrane in live chromaffin cells. Proc Natl Acad Sci U S A. 2013; 110:14249–54. [PubMed: 23940346]
66. Wu Z, Bello OD, Thiyagarajan S, Auclair SM, Vennekate W, Krishnakumar SS, O'Shaughnessy B, Karatekin E. Dilation of fusion pores by crowding of SNARE proteins. Elife. 2017:6.
67. Bao H, et al. Dynamics and number of trans-SNARE complexes determine nascent fusion pore properties. Nature. 2018; 554:260–263. [PubMed: 29420480]
68. Monck JR, Alvarez de Toledo G, Fernandez JM. Tension in secretory granule membranes causes extensive membrane transfer through the exocytotic fusion pore. Proc Natl Acad Sci U S A. 1990; 87:7804–7808. [PubMed: 2235997]

69. Kesavan J, Borisovska M, Bruns D. v-SNARE actions during Ca^{2+}-triggered exocytosis. Cell. 2007; 131:351–63. [PubMed: 17956735]
70. Walter AM, Wiederhold K, Bruns D, Fasshauer D, Sorensen JB. Synaptobrevin N-terminally bound to syntaxin-SNAP-25 defines the primed vesicle state in regulated exocytosis. J Cell Biol. 2010; 188:401–13. [PubMed: 20142423]
71. Zenisek D, Steyer JA, Feldman ME, Almers W. A membrane marker leaves synaptic vesicles in milliseconds after exocytosis in retinal bipolar cells. Neuron. 2002; 35:1085–97. [PubMed: 12354398]
72. Taraska JW, Almers W. Bilayers merge even when exocytosis is transient. Proc Natl Acad Sci U S A. 2004; 101:8780–5. [PubMed: 15173592]
73. Taraska JW, Perrais D, Ohara-Imaizumi M, Nagamatsu S, Almers W. Secretory granules are recaptured largely intact after stimulated exocytosis in cultured endocrine cells. Proc Natl Acad Sci U S A. 2003; 100:2070–2075. [PubMed: 12538853]
74. Axelrod D. Carbocyanine dye orientation in red cell membrane studied by microscopic fluorescence polarization. Biophys J. 1979; 26:557–73. [PubMed: 263688]
75. Anantharam A, Axelrod D, Holz RW. Polarized TIRFM reveals changes in plasma membrane topology before and during granule fusion. Cell Mol Neurobiol. 2010; 30:1343–9. [PubMed: 21061164]
76. Fernández-Chacón R, Alvarez de Toledo G. Cytosolic calcium facilitates release of secretory products after exocytotic vesicle fusion. FEBS Lett. 1995; 363:221– 225. [PubMed: 7737406]
77. Zhou Z, Misler S, Chow RH. Rapid fluctuations in transmitter release from single vesicles in bovine adrenal chromaffin cells. Biophys J. 1996; 70:1543–1552. [PubMed: 8785312]
78. Alés E, Tabares L, Poyato JM, Valero V, Lindau M, Alvarez de Toledo G. High calcium concentrations shift the mode of exocytosis to the kiss-and-run mechanism. Nat Cell Biol. 1999; 1:40–4. [PubMed: 10559862]
79. Geppert M, Goda Y, Hammer RE, Li C, Rosahl TW, Stevens CF, Sudhof TC. Synaptotagmin I: a major Ca2+ sensor for transmitter release at a central synapse. Cell. 1994; 79:717–27. [PubMed: 7954835]
80. Wang CT, Grishanin R, Earles CA, Chang PY, Martin TF, Chapman ER, Jackson MB. Synaptotagmin modulation of fusion pore kinetics in regulated exocytosis of dense-core vesicles. Science. 2001; 294:1111–1115. [PubMed: 11691996]
81. Bai J, Wang CT, Richards DA, Jackson MB, Chapman ER. Fusion pore dynamics are regulated by synaptotagmin*t-SNARE interactions. Neuron. 2004; 41:929–42. [PubMed: 15046725]
82. Zhu D, Zhou W, Liang T, Yang F, Zhang RY, Wu ZX, Xu T. Synaptotagmin I and IX function redundantly in controlling fusion pore of large dense core vesicles. Biochem Biophys Res Commun. 2007; 361:922–7. [PubMed: 17686463]
83. Segovia M, et al. Push-and-pull regulation of the fusion pore by synaptotagmin-7. Proc Natl Acad Sci U S A. 2010; 107:19032–7. [PubMed: 20956309]
84. Rao TC, Passmore DR, Peleman AR, Das M, Chapman ER, Anantharam A. Distinct fusion properties of synaptotagmin-1 and synaptotagmin-7 bearing dense core granules. Mol Biol Cell. 2014; 25:2416–27. [PubMed: 24943843]
85. Bendahmane M, et al. The synaptotagmin C2B domain calcium-binding loops modulate the rate of fusion pore expansion. Mol Biol Cell. 2018
86. Fisher RJ, Pevsner J, Burgoyne RD. Control of fusion pore dynamics during exocytosis by Munc18. Science. 2001; 291:875–8. [PubMed: 11157167]
87. Gulyas-Kovacs A, de Wit H, Milosevic I, Kochubey O, Toonen R, Klingauf J, Verhage M, Sorensen JB. Munc18–1: sequential interactions with the fusion machinery stimulate vesicle docking and priming. J Neurosci. 2007; 27:8676–86. [PubMed: 17687045]
88. Archer DA, Graham ME, Burgoyne RD. Complexin Regulates the Closure of the Fusion Pore during Regulated Vesicle Exocytosis. J Biol Chem. 2002; 277:18249–52. [PubMed: 11929859]
89. Cai H, Reim K, Varoqueaux F, Tapechum S, Hill K, Sorensen JB, Brose N, Chow RH. Complexin II plays a positive role in Ca2+-triggered exocytosis by facilitating vesicle priming. Proc Natl Acad Sci U S A. 2008; 105:19538–43. [PubMed: 19033464]

90. Dhara M, et al. Complexin synchronizes primed vesicle exocytosis and regulates fusion pore dynamics. J Cell Biol. 2014; 204:1123–40. [PubMed: 24687280]
91. Logan T, Bendor J, Toupin C, Thorn K, Edwards RH. alpha-Synuclein promotes dilation of the exocytotic fusion pore. Nat Neurosci. 2017; 20:681–689. [PubMed: 28288128]
92. Constable JR, Graham ME, Morgan A, Burgoyne RD. Amisyn regulates exocytosis and fusion pore stability by both syntaxin-dependent and syntaxin-independent mechanisms. J Biol Chem. 2005; 280:31615–23. [PubMed: 16033762]
93. Collins SC, et al. Increased Expression of the Diabetes Gene SOX4 Reduces Insulin Secretion by Impaired Fusion Pore Expansion. Diabetes. 2016; 65:1952–61. [PubMed: 26993066]
94. Weiss AN, Bittner MA, Holz RW, Axelrod D. Protein mobility within secretory granules. Biophys J. 2014; 107:16–25. [PubMed: 24988337]
95. Perrais D, Kleppe IC, Taraska JW, Almers W. Recapture after exocytosis causes differential retention of protein in granules of bovine chromaffin cells. J Physiol. 2004; 560:413–28. [PubMed: 15297569]
96. Weiss AN, Anantharam A, Bittner MA, Axelrod D, Holz RW. Lumenal protein within secretory granules affects fusion pore expansion. Biophys J. 2014; 107:26–33. [PubMed: 24988338]
97. de Wit J, Toonen RF, Verhage M. Matrix-dependent local retention of secretory vesicle cargo in cortical neurons. J Neurosci. 2009; 29:23–37. [PubMed: 19129381]
98. Bohannon KP, Bittner MA, Lawrence DA, Axelrod D, Holz RW. Slow fusion pore expansion creates a unique reaction chamber for co-packaged cargo. J Gen Physiol. 2017; 149:921–934. [PubMed: 28882880]
99. Hell SW, Wichmann J. Breaking the diffraction resolution limit by stimulated emission: stimulated-emission-depletion fluorescence microscopy. Opt Lett. 1994; 19:780–2. [PubMed: 19844443]
100. Chiang HC, et al. Post-fusion structural changes and their roles in exocytosis and endocytosis of dense-core vesicles. Nat Commun. 2014; 5:3356. [PubMed: 24561832]
101. Lollike K, Borregaard N, Lindau M. Capacitance flickers and pseudoflickers of small granules, measured in the cell-attached configuration. Biophys J. 1998; 75:53–9. [PubMed: 9649367]
102. Allersma MW, Wang L, Axelrod D, Holz RW. Visualization of regulated exocytosis with a granule-membrane probe using total internal reflection microscopy. Mol Biol Cell. 2004; 15:4658–68. [PubMed: 15282339]
103. Wen PJ, et al. Actin dynamics provides membrane tension to merge fusing vesicles into the plasma membrane. Nat Commun. 2016; 7:12604. [PubMed: 27576662]
104. Berberian K, Torres AJ, Fang Q, Kisler K, Lindau M. F-actin and myosin II accelerate catecholamine release from chromaffin granules. J Neurosci. 2009; 29:863–70. [PubMed: 19158310]
105. Gasman S, Chasserot-Golaz S, Malacombe M, Way M, Bader MF. Regulated exocytosis in neuroendocrine cells: a role for subplasmalemmal Cdc42/N-WASP-induced actin filaments. Mol Biol Cell. 2004; 15:520–31. [PubMed: 14617808]
106. Fesce R, Grohovaz F, Valtorta F, Meldolesi J. Neurotransmitter release: fusion or “kiss-and-run”? Trends Cell Biol. 1994; 4:1–4. [PubMed: 14731821]
107. Shin W, et al. Visualization of Membrane Pore in Live Cells Reveals a Dynamic-Pore Theory Governing Fusion and Endocytosis. Cell. 2018
108. Gubernator NG, et al. Fluorescent false neurotransmitters visualize dopamine release from individual presynaptic terminals. Science. 2009; 324:1441–4. [PubMed: 19423778]
109. Kozlov MM, Markin VS. Possible mechanism of membrane fusion. Biofizika. 1983; 28:242–7. [PubMed: 6849992]
110. Markin VS, Kozlov MM, Borovjagin VL. On the theory of membrane fusion. The stalk mechanism. Gen Physiol Biophys. 1984; 3:361–77. [PubMed: 6510702]
111. Kozlov MM, Leikin SL, Chernomordik LV, Markin VS, Chizmadzhev YA. Stalk mechanism of vesicle fusion. Intermixing of aqueous contents. Eur Biophys J. 1989; 17:121–9. [PubMed: 2792021]

112. Kozlovsky Y, Chernomordik LV, Kozlov MM. Lipid intermediates in membrane fusion: formation, structure, and decay of hemifusion diaphragm. Biophys J. 2002; 83:2634–51. [PubMed: 12414697]
113. Kemble GW, Danieli T, White JM. Lipid-anchored hemagglutinin promotes hemifusion, not complete fusion. Cell. 1994; 76:383–391. [PubMed: 8293471]
114. Armstrong RT, Kushnir AS, White JM. The transmembrane domain of influenza hemagglutinin exhibits a stringent length requirement to support the hemifusion to fusion transition. J Cell Biol. 2000; 151:425–37. [PubMed: 11038188]
115. Qiao H, Armstrong RT, Melikyan GB, Cohen FS, White JM. A specific point mutant at position 1 of the influenza hemagglutinin fusion peptide displays a hemifusion phenotype. Mol Biol Cell. 1999; 10:2759–69. [PubMed: 10436026]
116. Xu Y, Zhang F, Su Z, McNew JA, Shin YK. Hemifusion in SNARE-mediated membrane fusion. Nat Struct Mol Biol. 2005; 12:417–22. [PubMed: 15821745]
117. Liu T, Wang T, Chapman ER, Weisshaar JC. Productive hemifusion intermediates in fast vesicle fusion driven by neuronal SNAREs. Biophys J. 2008; 94:1303–14. [PubMed: 17951297]
118. Hernandez JM, et al. Membrane fusion intermediates via directional and full assembly of the SNARE complex. Science. 2012; 336:1581–4. [PubMed: 22653732]
119. Diao J, et al. Synaptic proteins promote calcium-triggered fast transition from point contact to full fusion. Elife. 2012; 1:e00109. [PubMed: 23240085]
120. Kasson PM, Kelley NW, Singhal N, Vrljic M, Brunger AT, Pande VS. Ensemble molecular dynamics yields submillisecond kinetics and intermediates of membrane fusion. Proc Natl Acad Sci U S A. 2006; 103:11916–21. [PubMed: 16880392]
121. Kasson PM, Lindahl E, Pande VS. Atomic-resolution simulations predict a transition state for vesicle fusion defined by contact of a few lipid tails. PLoS Comput Biol. 2010; 6:e1000829. [PubMed: 20585620]
122. Nishizawa M, Nishizawa K. Molecular dynamics simulation analysis of membrane defects and pore propensity of hemifusion diaphragms. Biophys J. 2013; 104:1038–48. [PubMed: 23473486]
123. Risselada HJ, Grubmuller H. How SNARE molecules mediate membrane fusion: recent insights from molecular simulations. Curr Opin Struct Biol. 2012; 22:187–96. [PubMed: 22365575]
124. Zhao WD, et al. Hemi-fused structure mediates and controls fusion and fission in live cells. Nature. 2016; 534:548–52. [PubMed: 27309816]
125. James DJ, Martin TF. CAPS and Munc13: CATCHRs that SNARE Vesicles. Front Endocrinol (Lausanne). 2013; 4:187. [PubMed: 24363652]
126. Gandasi NR, Barg S. Contact-induced clustering of syntaxin and munc18 docks secretory granules at the exocytosis site. Nat Commun. 2014; 5:3914. [PubMed: 24835618]
127. Brose N, Petrenko AG, Südhof TC, Jahn R. Synaptotagmin: a calcium sensor on the synaptic vesicle surface. Science. 1992; 256:1021–1025. [PubMed: 1589771]
128. McMahon HT, Missler M, Li C, Sudhof TC. Complexins: cytosolic proteins that regulate SNAP receptor function. Cell. 1995; 83:111–9. [PubMed: 7553862]
129. Maximov A, Tang J, Yang X, Pang ZP, Sudhof TC. Complexin controls the force transfer from SNARE complexes to membranes in fusion. Science. 2009; 323:516–21. [PubMed: 19164751]
130. Betz A, Ashery U, Rickmann M, Augustin I, Neher E, Südhof TC, Rettig J, Brose N. Munc13-1 is a presynaptic phorbol ester receptor that enhances neurotransmitter release. Neuron. 1998; 21:123–136. [PubMed: 9697857]
131. Kreutzberger AJB, Kiessling V, Liang B, Seelheim P, Jakhanwal S, Jahn R, Castle JD, Tamm LK. Reconstitution of calcium-mediated exocytosis of dense-core vesicles. Sci Adv. 2017; 3:e1603208. [PubMed: 28776026]
132. Rothman JE, Krishnakumar SS, Grushin K, Pincet F. Hypothesis - buttressed rings assemble, clamp, and release SNAREpins for synaptic transmission. FEBS Lett. 2017; 591:3459–3480. [PubMed: 28983915]
133. Anantharam A, Onoa B, Edwards RH, Holz RW, Axelrod D. Localized topological changes of the plasma membrane upon exocytosis visualized by polarized TIRFM. J Cell Biol. 2010; 188:415–28. [PubMed: 20142424]

134. Llobet A, Wu M, Lagnado L. The mouth of a dense-core vesicle opens and closes in a concerted action regulated by calcium and amphiphysin. J Cell Biol. 2008; 182:1017–28. [PubMed: 18779374]
135. van den Bogaart G, Lang T, Jahn R. Microdomains of SNARE proteins in the plasma membrane. Curr Top Membr. 2013; 72:193–230. [PubMed: 24210431]
136. Sieber JJ, Willig KI, Heintzmann R, Hell SW, Lang T. The SNARE motif is essential for the formation of syntaxin clusters in the plasma membrane. Biophys J. 2006; 90:2843–51. [PubMed: 16443657]
137. Sieber JJ, et al. Anatomy and dynamics of a supramolecular membrane protein cluster. Science. 2007; 317:1072–6. [PubMed: 17717182]
138. Knowles MK, Barg S, Wan L, Midorikawa M, Chen X, Almers W. Single secretory granules of live cells recruit syntaxin-1 and synaptosomal associated protein 25 (SNAP-25) in large copy numbers. Proc Natl Acad Sci U S A. 2010; 107:20810–5. [PubMed: 21076040]
139. Pertsinidis A, et al. Ultrahigh-resolution imaging reveals formation of neuronal SNARE/Munc18 complexes in situ. Proc Natl Acad Sci U S A. 2013; 110:E2812–20. [PubMed: 23821748]
140. Yang L, et al. Secretory vesicles are preferentially targeted to areas of low molecular SNARE density. PLoS One. 2012; 7:e49514. [PubMed: 23166692]
141. Barg S, Knowles MK, Chen X, Midorikawa M, Almers W. Syntaxin clusters assemble reversibly at sites of secretory granules in live cells. Proc Natl Acad Sci U S A. 2010; 107:20804–9. [PubMed: 21076041]
142. Ma C, Li W, Xu Y, Rizo J. Munc13 mediates the transition from the closed syntaxin-Munc18 complex to the SNARE complex. Nat Struct Mol Biol. 2011; 18:542–9. [PubMed: 21499244]
143. Lang T, Bruns D, Wenzel D, Riedel D, Holroyd P, Thiele C, Jahn R. SNAREs are concentrated in cholesterol-dependent clusters that define docking and fusion sites for exocytosis. EMBO J. 2001; 20:2202–13. [PubMed: 11331586]
144. Ullrich A, Bohme MA, Schoneberg J, Depner H, Sigrist SJ, Noe F. Dynamical Organization of Syntaxin-1A at the Presynaptic Active Zone. PLoS Comput Biol. 2015; 11:e1004407. [PubMed: 26367029]
145. Sharma S, Lindau M. t-SNARE Transmembrane Domain Clustering Modulates Lipid Organization and Membrane Curvature. J Am Chem Soc. 2017; 139:18440–18443. [PubMed: 29231734]
146. Yang ST, Kreutzberger AJB, Lee J, Kiessling V, Tamm LK. The role of cholesterol in membrane fusion. Chem Phys Lipids. 2016; 199:136–143. [PubMed: 27179407]
147. Wasser CR, Ertunc M, Liu X, Kavalali ET. Cholesterol-dependent balance between evoked and spontaneous synaptic vesicle recycling. J Physiol. 2007; 579:413–29. [PubMed: 17170046]
148. Rituper B, Flasker A, Gucek A, Chowdhury HH, Zorec R. Cholesterol and regulated exocytosis: a requirement for unitary exocytotic events. Cell Calcium. 2012; 52:250–8. [PubMed: 22726879]
149. Kreutzberger AJ, Kiessling V, Tamm LK. High cholesterol obviates a prolonged hemifusion intermediate in fast SNARE-mediated membrane fusion. Biophys J. 2015; 109:319–29. [PubMed: 26200867]
150. Chen Z, Rand RP. The influence of cholesterol on phospholipid membrane curvature and bending elasticity. Biophys J. 1997; 73:267–76. [PubMed: 9199791]
151. Somanath S, Barg S, Marshall C, Silwood CJ, Turner MD. High extracellular glucose inhibits exocytosis through disruption of syntaxin 1A-containing lipid rafts. Biochem Biophys Res Commun. 2009; 389:241–6. [PubMed: 19716806]
152. Stratton BS, et al. Cholesterol Increases the Openness of SNARE-Mediated Flickering Fusion Pores. Biophys J. 2016; 110:1538–1550. [PubMed: 27074679]
153. Kolay S, Basu U, Raghu P. Control of diverse subcellular processes by a single multi-functional lipid phosphatidylinositol 4,5-bisphosphate [PI(4,5)P2]. Biochem J. 2016; 473:1681–92. [PubMed: 27288030]
154. van den Bogaart G, et al. Membrane protein sequestering by ionic protein-lipid interactions. Nature. 2011; 479:552–5. [PubMed: 22020284]

155. Khelashvili G, Galli A, Weinstein H. Phosphatidylinositol 4,5-biphosphate (PIP(2)) lipids regulate the phosphorylation of syntaxin N-terminus by modulating both its position and local structure. Biochemistry. 2012; 51:7685–98. [PubMed: 22950482]

156. Sharma S, Kim BN, Stansfeld PJ, Sansom MS, Lindau M. A Coarse Grained Model for a Lipid Membrane with Physiological Composition and Leaflet Asymmetry. PLoS One. 2015; 10:e0144814. [PubMed: 26659855]

157. Lam AD, Tryoen-Toth P, Tsai B, Vitale N, Stuenkel EL. SNARE-catalyzed fusion events are regulated by Syntaxin1A-lipid interactions. Mol Biol Cell. 2008; 19:485–97. [PubMed: 18003982]

158. Gong LW, Di Paolo G, Diaz E, Cestra G, Diaz ME, Lindau M, De Camilli P, Toomre D. Phosphatidylinositol phosphate kinase type I gamma regulates dynamics of large dense-core vesicle fusion. Proc Natl Acad Sci U S A. 2005; 102:5204–9. [PubMed: 15793002]

159. Milosevic I, Sorensen JB, Lang T, Krauss M, Nagy G, Haucke V, Jahn R, Neher E. Plasmalemmal phosphatidylinositol-4,5-bisphosphate level regulates the releasable vesicle pool size in chromaffin cells. J Neurosci. 2005; 25:2557–65. [PubMed: 15758165]

160. Kabachinski G, Yamaga M, Kielar-Grevstad DM, Bruinsma S, Martin TF. CAPS and Munc13 utilize distinct PIP2-linked mechanisms to promote vesicle exocytosis. Mol Biol Cell. 2014; 25:508–21. [PubMed: 24356451]

161. Walter AM, et al. Phosphatidylinositol 4,5-bisphosphate optical uncaging potentiates exocytosis. Elife. 2017:6.

162. Khuong TM, et al. Synaptic PI(3,4,5)P3 is required for Syntaxin1A clustering and neurotransmitter release. Neuron. 2013; 77:1097–108. [PubMed: 23522045]

163. Aoyagi K, Sugaya T, Umeda M, Yamamoto S, Terakawa S, Takahashi M. The activation of exocytotic sites by the formation of phosphatidylinositol 4,5-bisphosphate microdomains at syntaxin clusters. J Biol Chem. 2005; 280:17346–52. [PubMed: 15741173]

164. James DJ, Khodthong C, Kowalchyk JA, Martin TF. Phosphatidylinositol 4,5-bisphosphate regulates SNARE-dependent membrane fusion. J Cell Biol. 2008; 182:355–66. [PubMed: 18644890]

165. Honigmann A, et al. Phosphatidylinositol 4,5-bisphosphate clusters act as molecular beacons for vesicle recruitment. Nat Struct Mol Biol. 2013; 20:679–86. [PubMed: 23665582]

166. Ji C, Fan F, Lou X. Vesicle Docking Is a Key Target of Local PI(4,5)P2 Metabolism in the Secretory Pathway of INS-1 Cells. Cell Rep. 2017; 20:1409–1421. [PubMed: 28793264]

167. Omar-Hmeadi M, Gandasi NR, Barg S. PtdIns(4,5)P2 is not required for secretory granule docking. Traffic. 2018

168. Robertson JD. The ultrastructure of a reptilian myoneural junction. J Biophys Biochem Cytol. 1956; 2:381–94. [PubMed: 13357502]

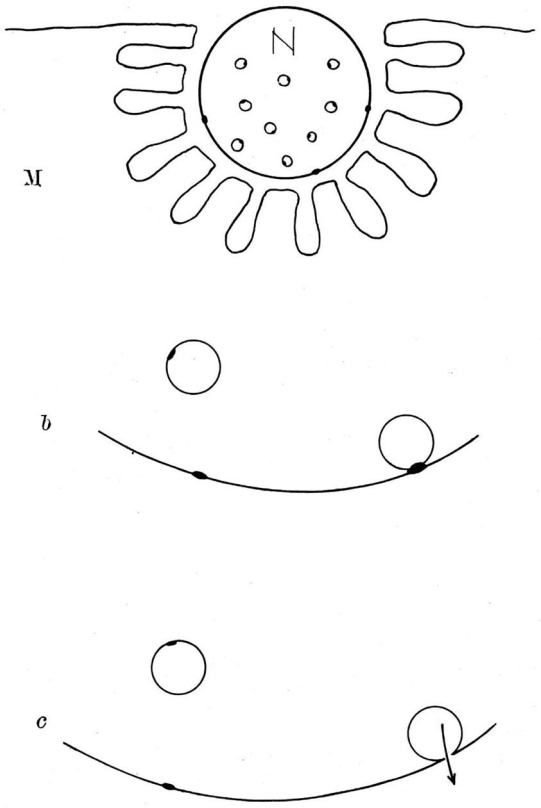

FIG. 5. — Schéma expliquant le caractère quantal de décharge d'Ach d'une terminaison d'un nerf moteur (N). M : fibre musculaire avec replis jonctionnels (*cf.* Robertson, 1956). On pense que le transmetteur est préformé dans les microsomes intracellulaires, qui après collision critique avec la membrane du nerf, libèrent leur contenu en Ach dans l'espace intersynaptique. Ce phénomène est illustré en *b* et *c* et l'on peut supposer qu'il se produit quand certaines molécules réactives (figurées par des points) des deux surfaces se rencontrent.

Fig. 1.

Diagram explaining the quantal discharge character of Ach at a motor nerve terminal (N). M: muscle fiber with junctional folds (see Robertson, 1956 [168]). The transmitter is believed to be preformed in intracellular microsomes, which after critical collision with the nerve membrane, release their Ach contents into the intersynaptic space. This phenomenon is illustrated in b and c and it can be assumed that it occurs when certain reactive molecules (represented by dots) of the two surfaces meet. From [3].

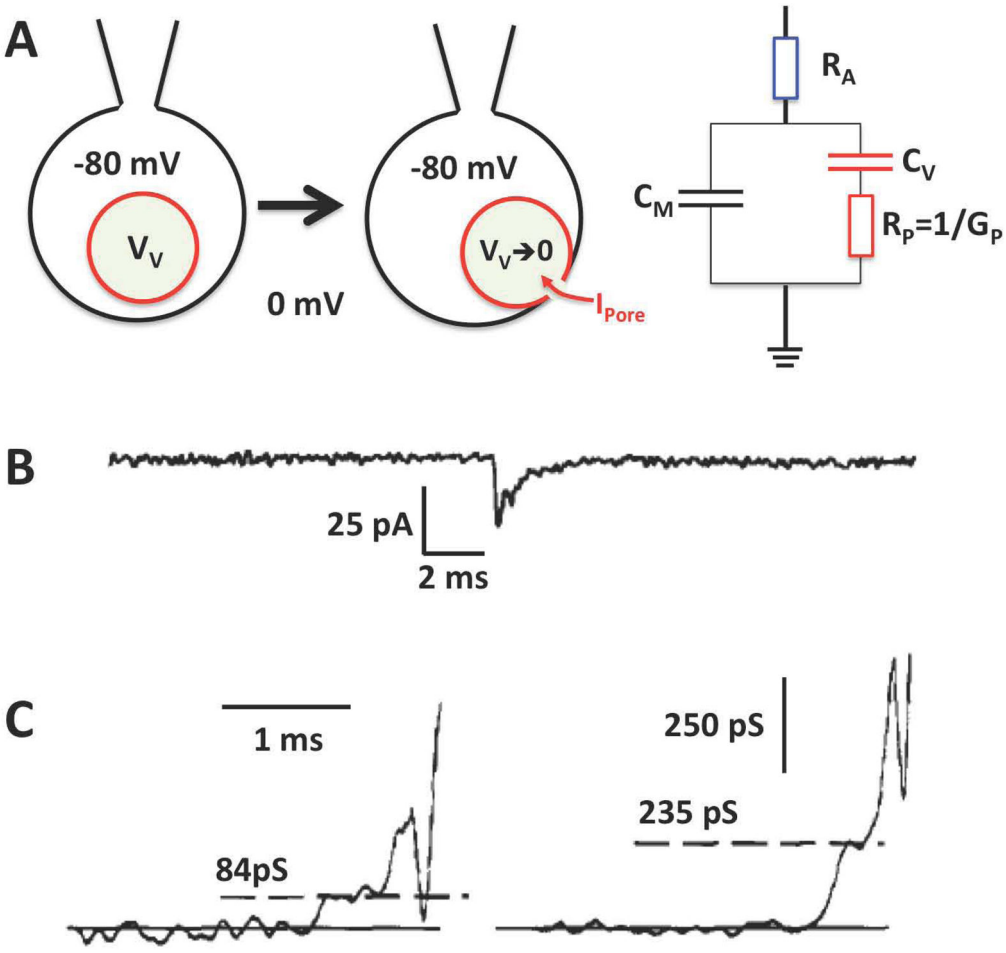

Fig. 2.

Initial fusion pore conductance from analysis of current transients. (A) Upon fusion the capacitance Cv of the vesicle is added to the plasma membrane (C_M) and any intravesicular potential V_V is rapidly discharged by the current I_{Pore} that flows across the fusion pore conductance Gp. The initial V_V is obtained from the integrated charge of I_{Pore} and the C_V. C_V is the difference of C_M before the fusion event and after fusion event. C_M is measured periodically by applying a sine wave voltage to determine the equivalent circuit parameters. R_A is the access resistance from the pipette tip. (B) A typical current transient measured at −80 mV holding potential. (C) Two representative fusion events showing different initial G_P. Modified after reference [8].

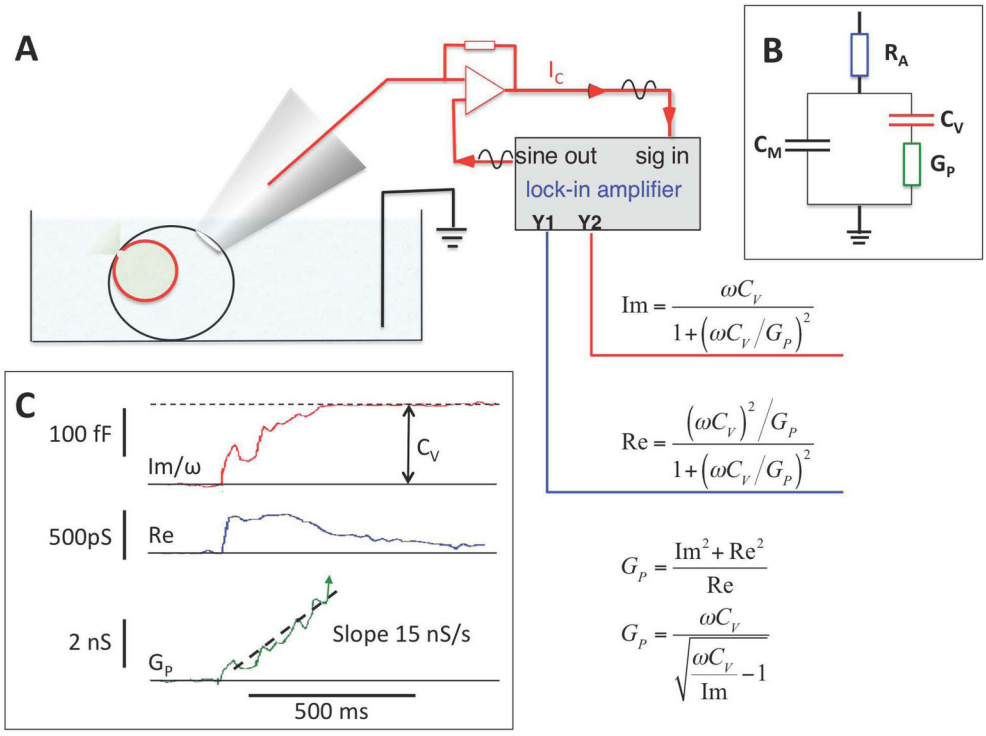

Fig. 3.

Whole cell capacitance measurements of fusion pore dynamics in cells with large vesicles. (A) Whole cell configuration using the lock-in amplifier technique and equations used for analysis. (B) Minimal equivalent circuit for analysis of fusion pore conductance with access (pipette) resistance R_A, membrane capacitance C_M, vesicle capacitance C_V, and fusion pore conductance G_P. (C) Recording of fusion pore expansion in a horse eosinophil. When the fusion pore conductance increases, the phase shifted current component (Im/ω, red) increases gradually to the full vesicle capacitance C_V while the in-phase component (Re, blue) shows a transient increase. G_P can be calculated from Im and Re or from Im and C_V as indicated. G_P shows a fluctuating increase with an average slope of ~15 nS/s. Data from reference [8].

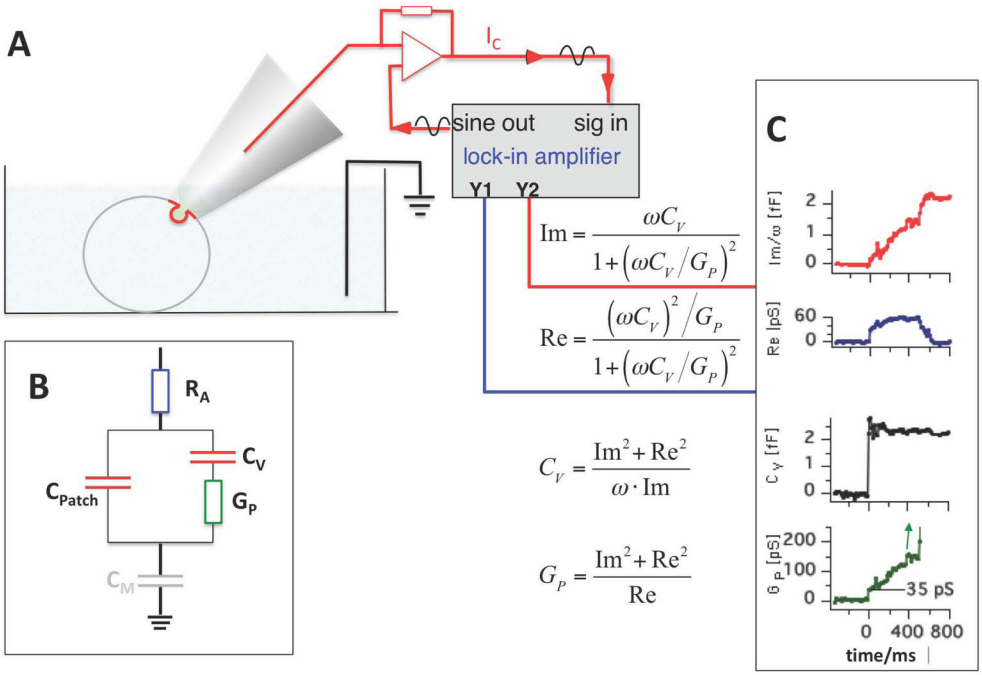

Fig. 4.

Cell attached capacitance measurements of fusion pore dynamics in cells with small vesicles. (A) Cell attached configuration using the lock-in amplifier technique. (B) Minimal equivalent circuit for analysis of fusion pore conductance with components R_A, C_M, C_V, and G_P. In this configuration the measured capacitance is that of the patch (C_{Patch}). C_M is negligible because it is much larger than C_{Patch} and enters with its reciprocal value. (C) Recording of fusion pore opening from a human neutrophil [11]. G_P rises from an initial value as small as 35 pS. C_V was calculated from Re and Im as indicated.

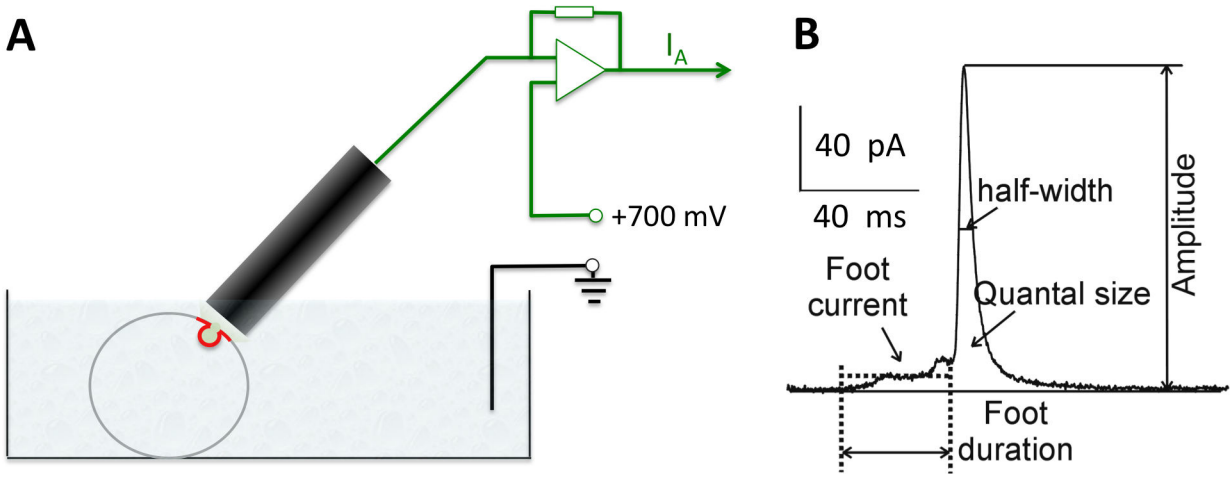

Fig. 5.

Amperometric measurement of fusion pore dynamics. (A) A CFM is placed close to the cell and a voltage of typically 700 mV is applied. (B) Amperometric current from a single fusion event in a chromaffin cell [54]. The amperometric current reports the flux of catecholamine molecules from the vesicle. Amperometric spikes are typically quantified by quantal size, half width, mean foot current and foot duration as indicated. The foot current reports fusion pore properties as shown in Fig. 6.

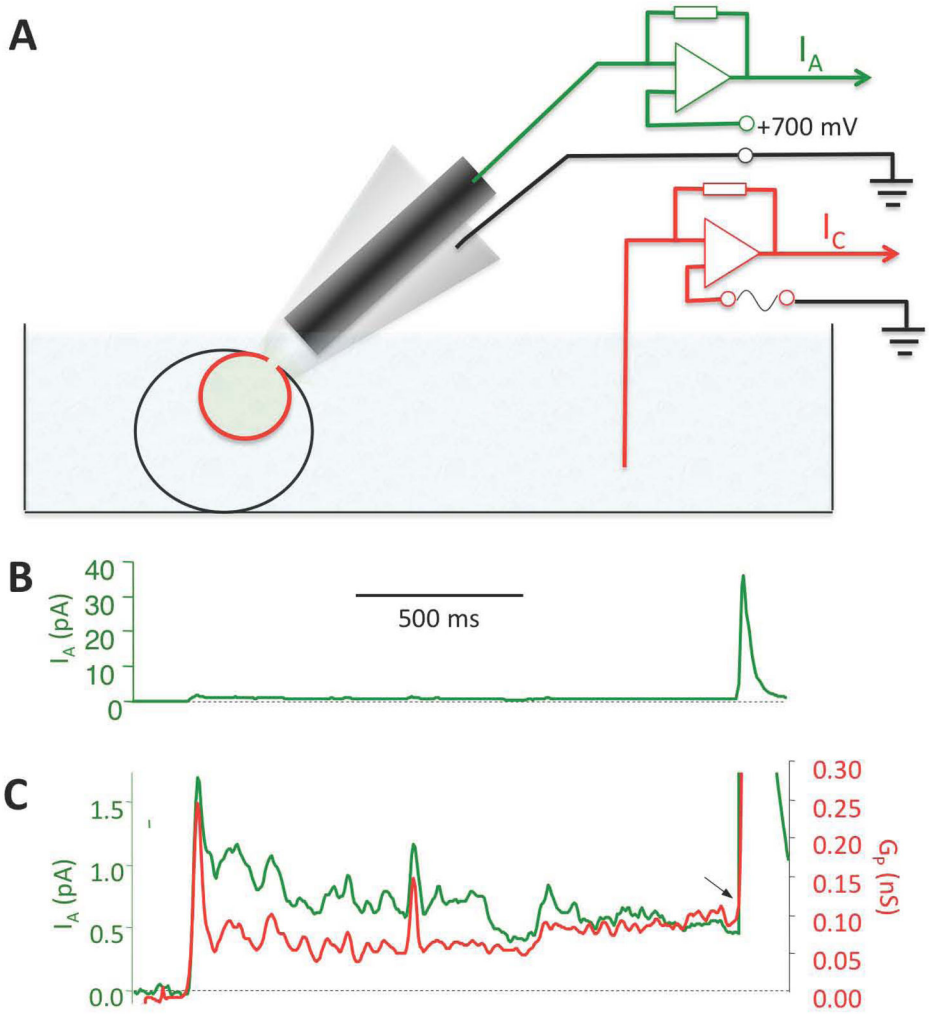

Fig. 6.

(A) Patch amperometry records simultaneously fusion pore conductance by cell attached capacitance measurement and catecholamine release by amperometry with a CFM inserted into the patch pipette together with the reference electrode. The sine wave for capacitance measurement is applied to the bath electrode. (B) Measurement of a single fusion event with extremely long amperometric foot signal. (C) Foot current fluctuations (green trace) are synchronous with G_P fluctuations (red trace).

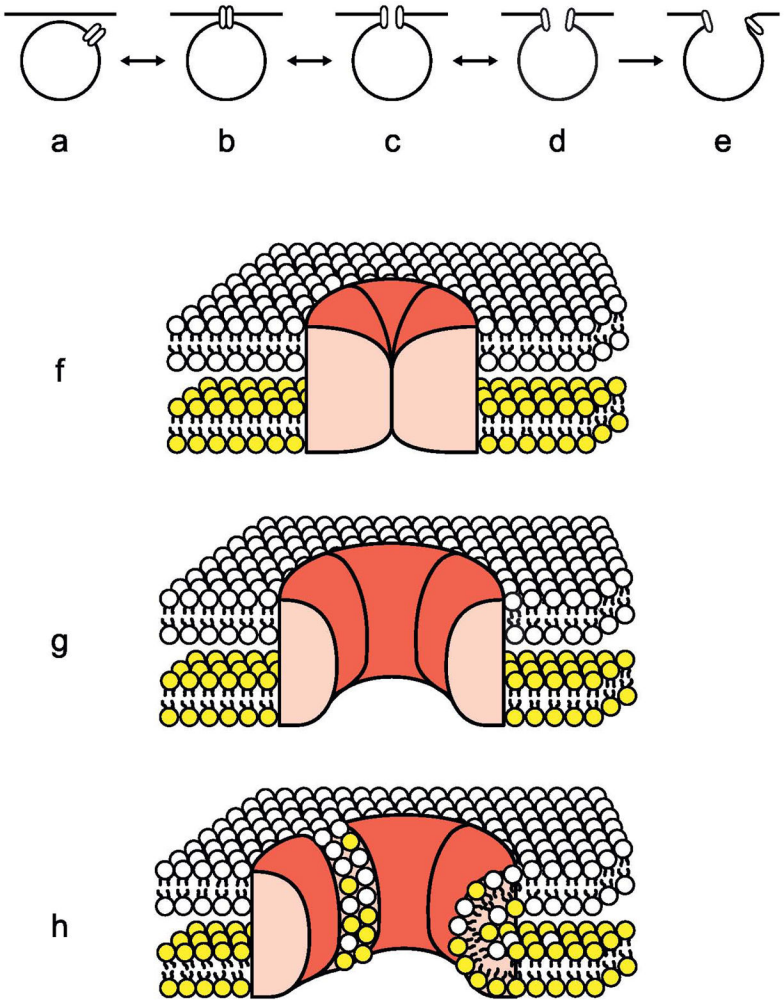

Fig. 7.

Hypothetical steps in exocytosis. A–E illustrate the hypothesis where a proteinaceous fusion pore is formed, expands and eventually proceeds to full fusion. F–H show a section through the hypothetical fusion pore complex and the position of that complex in the two lipid bilayers of the plasma and vesicle membranes. Once the pore has opened, lipid molecules can diffuse along the amphipathic surfaces exposed between the fusion pore subunits. The entry of lipid molecules between the subunits causes the pore to dilate. Redrawn after [22]

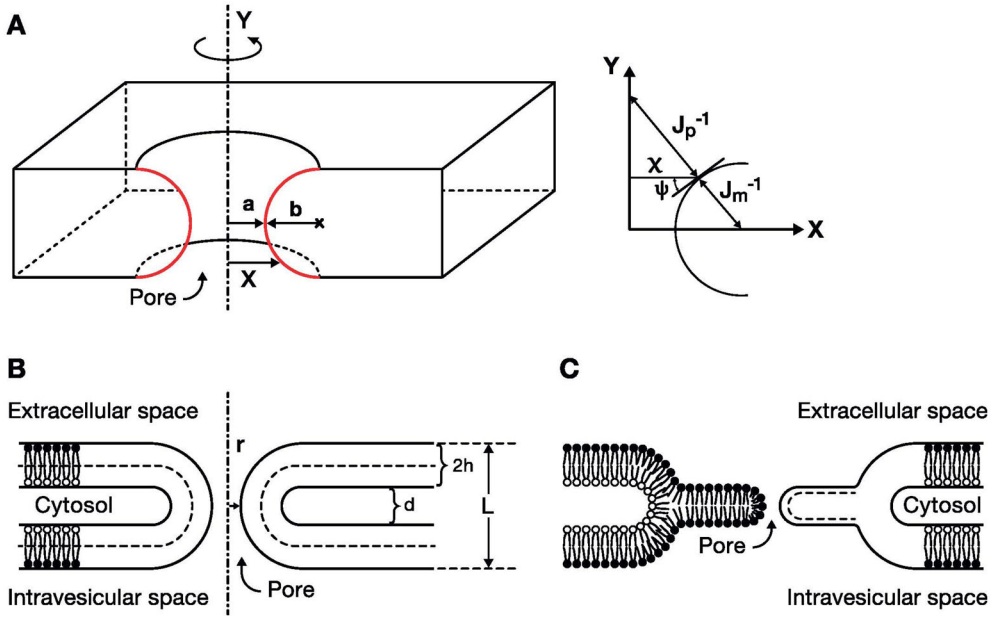

Fig. 8.

Geometry of a lipidic pore that is generated by revolving the semicircles (red curves) about the axis of revolution, Y. a = radius of the narrowest part of the pore; b = radius of the generating semicircles; X = shortest distance between the axis of revolution and a point on the semicircle. Inset shows the same geometry with the angle and radii of curvatures. J_p^{-1} and J_m^{-1} are the parallel and meridional radii of curvature, respectively. ψ(x) is the angle between the tangent to the semicircle at the point (x, y) and the horizontal axis. (B) A pore spanning two bilayers and the space between them. h=monolayer thickness, d=interbilayer distance, L = pore length = 4h + d. (C) A pore spanning the single bilayer formed on hemifusion of the fusing bilayers (L = 2h). Modified after [27].

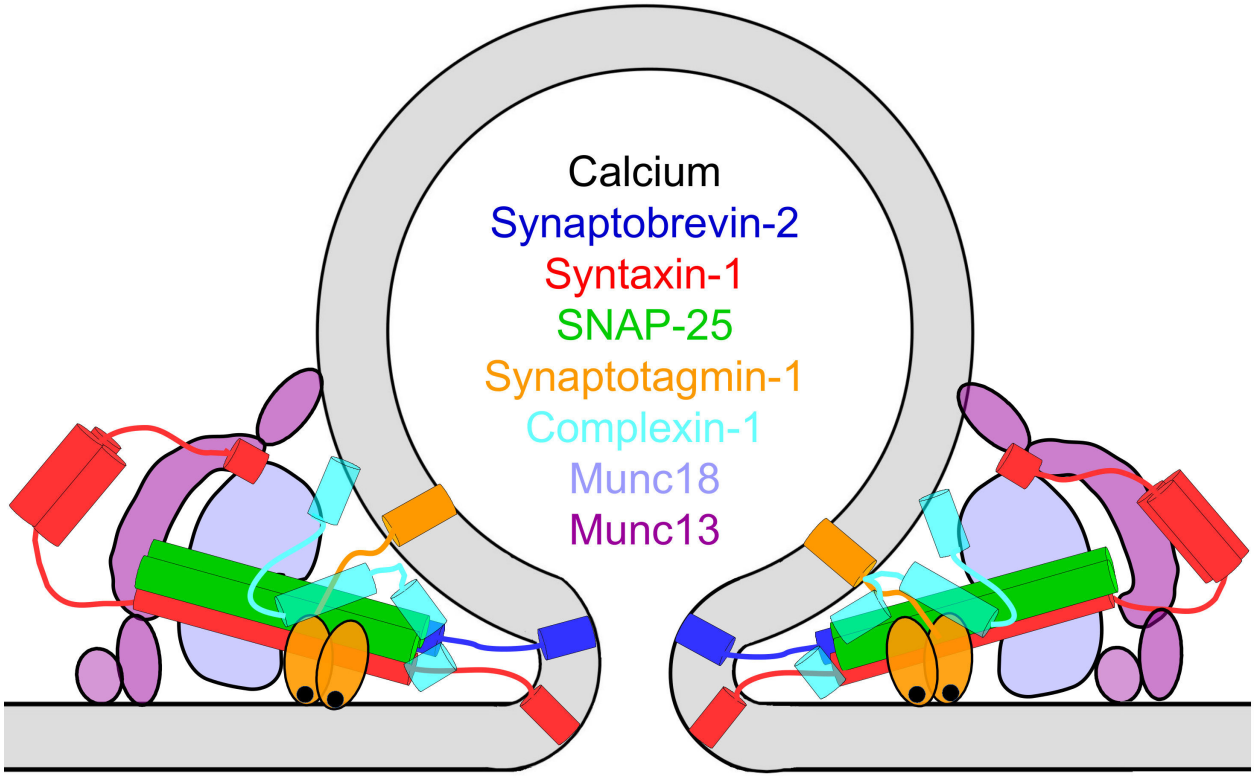

Fig. 9.

Schematic illustration of a proteolipidic fusion pore formed by SNAREs in cooperation with accessory proteins as indicated. The function of the various components is discussed in the text. Ca^{2+} ions are depicted as black dots.